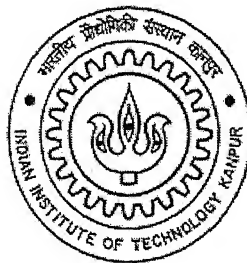


# **Kinematic Synthesis of Harmonic Drive Tooth Profile and Study of the Performance Characteristics**

A Thesis submitted  
in partial fulfillment of the requirements  
for the degree of  
**Master of Technology**

by

**Manchi Venkateswararao**



**Department of Mechanical Engineering  
Indian Institute of Technology, Kanpur  
India**

April 2005.

12 JUL 2005 / ME  
दुष्पातम का गीताथ कलकर पुस्तकालय  
भारतीय प्रोद्योगिकी संस्थान कानपुर  
बपानि ड० 152018



A152018

## **Acknowledgements**

A journey is easier when you travel together. Interdependence is certainly more valuable than independence. This thesis is the result of one year of work whereby I have been suggested and supported by many people. It is a pleasant aspect that I have now the opportunity to express my gratitude for all of them.

First, I express my sincere gratitude to my thesis supervisor Prof. Amitabha Ghosh for his continuous support and critical appraisal. He is responsible for involving me in this project in the first place. He showed me different ways to approach a research problem and the need to be persistent to accomplish any goal. His interest in research and his mission for providing 'only high-quality work even less', has made a deep impression on me. The confidence and dynamism with which he guided the work requires no elaboration. He directed me in writing academic papers and brought out the good ideas in me. Besides being an excellent supervisor, he is friendly towards his students. I am really glad that I have come to get know Prof. Ghosh in my life.

I am grateful to the institute, the INDIAN INSTITUTE OF TECHNOLOGY, Kanpur. I could complete this task by the facilities provided by the institute.

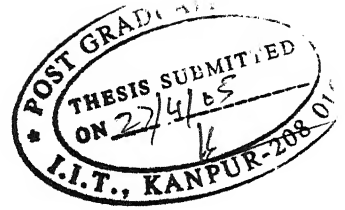
I am also greatly indebted to my close friends who took effort in providing me their extensive comments which had indirect impact on the quality of work. I thank them for having shared many of my experiences and thoughts throughout the year. Special thanks are due to Rishi Kumar Sharma, Vinod Kulkarni and Alok Kumar Singh for their extended help and brotherly advice. Additional energy and vitality is provided by friends Varanasi Jagannad, Ravi Kumar, Srinivasrao and Vinay Maruti.

Finally, I thank all whose direct and indirect support helped me in completing my thesis.

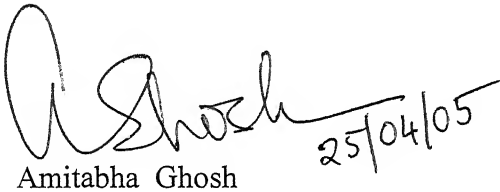
April, 2005

Manchi Venkateswararao

## CERTIFICATE



It is certified that work contained in the thesis entitled “**Kinematic Synthesis of Harmonic Drive Tooth Profile and Study of The Performance Characteristics**” by **Manchi Venkateswararao**, has been carried out under my supervision and that this work has not been submitted elsewhere for a degree.

  
Amitabha Ghosh

Professor

Department of Mechanical Engineering

I. I. T Kanpur.



*This thesis is dedicated to my grandmother*

*Manchi Ramakoteswaramma*

## **Abstract**

Harmonic drives are commonly used for achieving large transmission ratios using a compact device. These drives can also be extensively used for precise positioning applications. Generally standard tooth forms are chosen for the gears of such drives. Since the perfect gearing action is not ensured, such drives display certain amount of kinematic error, which is defined as the difference between the ideal and the actual angular positions of the output gear. When a definite rotation is given to the wave generator, it is expected that if the tooth profile is synthesized to ensure perfect gearing action i.e. the instantaneous transmission ratio remains constant, the kinematic error can be substantially reduced if not completely eliminated. This work deals with the kinematics of tooth engagement in harmonic drives with a view to achieve a constant value of instantaneous transmission ratios. It is known that the magnitude of kinematic error increases with reduction in transmission ratio. Therefore, this trend has also been investigated with synthesized tooth profiles. It has been found that the effect is less pronounced when synthesized profiles are used. The lengths of contact on both the circular spline teeth and the flexspline teeth are restricted to low values in case of standard harmonic drives with involute profiles; this tends to intensify the wearing action changing the geometry of teeth profiles in a short period of working life. A methodology has been proposed for synthesizing the tooth profiles not only for reducing the kinematic error but also to increase the lengths of contact thus, in turn, reducing the effect of wear on teeth profiles. The ideal kinematic error with involute tooth profiles for different gear ratios has been compared with that in case of synthesized profiles. The theoretical mechanical efficiency of harmonic drives with the synthesized and the involute teeth profiles is determined. The effect of gear ratio on mechanical efficiency is also presented. The contact stresses in the circular spline and the flexspline teeth are estimated using a finite element model. The Hertz stresses at the teeth contact with standard involute profiles and synthesized profiles are compared.

## Nomenclature

- CS = Circular spline
- $E$  = Elliptical shape of the flexspline after deformation
- $f$  = frictional force at the contact point
- $F$  = Initial shape of the flexspline (circular)
- FS = Flexible spline or flexspline
- $r$  = distance between contact point of teeth and the CS
- $R_p, r_p$  = Radii of pitch circles of the CS and the FS
- $R_b, r_b$  = Radii of base circles of the CS and the FS
- $T_{cs}$  = Number of teeth on the CS
- $P P'$  = Trace of a point  $P$  on the FS
- SC = The circular spline segment
- SF = The flexspline segment
- TT = Common tangent to the base circles of involute gearing
- $T_1 T_1$  = Common tangent to the teeth profiles
- WG = Wave generator
- $X_1 X_2$  = Tangent to an imaginary circle concentric to CS passing through contact point
- $x$  = Linear displacement of the CS
- $\gamma$  = Change in the angle of the normal at a point on the circle  $F$  for certain rotation of the WG
- $\psi$  = Small angular displacement of the WG in the counter clockwise direction
- $\rho$  = Transmission ratio
- $\theta$  = Slope of the profile at any instant with the tangent  $X_1 X_2$
- $\phi$  = Slope of the trace of the FS tooth at any instant with the tangent  $X_1 X_2$
- $\mu$  = Coefficient of friction
- $P_f$  = Energy lost due to friction at the interface
- $P_n$  = Normal acting at the contact point of teeth profiles
- $V_s$  = Sliding velocity of the FS teeth over the CS teeth
- $V_f$  = Velocity of the FS teeth.
- $V_c$  = Tangential velocity of the CS calculated at the contact point
- $t_1$  = Time at the starting of the engagement of the FS tooth with the CS tooth.
- $t_2$  = Time at the disengagement of the FS tooth from the CS tooth

# CONTENTS

## List of Figures

## List of Tables

### 1. Harmonic Drive

1.1 Introduction.....	1
1.2 The principle of operation.....	3
1.3 Performance features and applicability.....	3
1.4 Other mechanisms used for speed reduction.....	5
1.5 The state of harmonic drive technology.....	11
1.6 Kinematic error.....	13
1.7 Objectives .....	14

### 2. Kinematic Analysis and Synthesis.....15

2.1 Path traced by a point on the flexspline as the wave generator rotates.....	15
2.2 Kinematic analysis of drives with involute profile .....	17
2.3 Determination of the kinematic error.....	20
2.4 Synthesis of the teeth profiles.....	23
2.5 Comparison between the involute and the synthesized teeth profiles.....	27

### 3. Mechanical Efficiency.....31

3.1 Theoretical determination of mechanical efficiency.....	31
3.2 Effect of speed on mechanical efficiency.....	34
3.3 Effect of gear ratio on mechanical efficiency.....	37
3.4 The velocity profiles of the flexspline tooth.....	38

### 4. Contact Stresses.....44

4.1 Hertz stresses at teeth contact of drives with involute profiles.....	45
4.2 Hertz stresses at teeth contact of drives with synthesized profiles.....	48

### 5. Concluding remarks.....53

## References

## Appendix I

## List of figures

Fig. 1 Harmonic Drive

Fig. 2 Harmonic drive with disc type WG

Fig. 3 Worm and worm gear drive

Fig. 4 Cycloidal drive

Fig. 5 Motion of a point on the FS

Fig. 6 Change in the direction of normal of the FS tooth

Fig. 7 Internal gear pair

a. Internal gear and pinion

b. Detailed view

Fig. 8 The contact of the FS teeth with the CS teeth after the FS is deformed

Fig. 9 Forward motion of the FS tooth.

(a) Beginning of the forward motion of the FS tooth.

(b) End of the forward motion of the FS tooth.

Fig. 10 Teeth position before and after finite rotation of the WG

(a) Teeth position at the beginning of the rotation of the WG

(b) Teeth position after the rotation of the WG through an angle  $\psi$

Fig. 11 Kinematic error of Harmonic drives with involute profile for different gear ratios.

Fig. 12 Detailed view of kinematic error

Fig. 13 Displacement of circle A and circle B

Fig. 14 Approximate motion of the CS for the given motion the FS teeth

Fig. 15 The synthesized and the involute profiles.

Fig. 16a. Approximate motion of the CS for the given motion the FS teeth

Fig. 16b The final segments after extending the FS segment to meet the CS segment

Fig. 17 The synthesized and the involute profiles for an elliptical WG

Fig. 18 Circular spline teeth

Fig. 19 Forces acting at the interface of the teeth contact

Fig. 20 Variation of coefficient of friction with sliding velocity

Fig. 21(a) Variation of efficiency with the input speed for gear ratio 25 (over a short range)

Fig. 21(b) Variation of efficiency with the input speed for gear ratio 25 (over a large range)

Fig. 21(c) Mechanical efficiency of drive with involute and synthesized profiles (gear ratio 25)

Fig. 22 Variation of efficiency with increase in torque for gear ratio 25 (over a large range)

Fig. 23 Mechanical efficiency with different speed ratio (involute profile)

Fig. 24(a) Velocity of the FS tooth at the input speed 100 rpm

Fig. 24(b) Velocity of the FS tooth at the input speed 1500 rpm

Fig. 24(c) Velocity of the FS tooth at the input speed 5000 rpm

Fig. 24(d) Velocity of the FS tooth at the input speed 8000 rpm

Fig. 25(a) Velocity of the FS tooth at the input speed 100 rpm

Fig. 25(b) Velocity of the FS tooth at the input speed 1500 rpm

Fig. 25(c) Velocity of the FS tooth at the input speed 5000 rpm

Fig. 25(d) Velocity of the FS tooth at the input speed 8000 rpm

Fig. 26(a) Velocity of the FS tooth at the input speed 1500 rpm

Fig. 26(b) Velocity of the FS tooth at the input speed 8000 rpm

Fig. 27(a) The contact between the FS and the CS teeth at the starting of engagement

Fig. 27(b) Stress distribution at the start of the engagement

Fig. 27(c) The contact between the FS and the CS teeth at the middle of the engagement

Fig. 27(d) Stress distribution at the middle of the engagement

Fig. 27(e) The contact between the FS and the CS teeth at the end of the engagement

Fig. 27(f) Stresses distribution at the end of the engagement

Fig. 28(a) The contact between the FS and the CS teeth at the starting of the engagement

Fig. 28(b) Stress distribution at the start of the engagement

Fig. 28(c) The contact between the FS and the CS teeth at the middle of the engagement

Fig. 28(d) Stress distribution at the middle of the engagement

Fig. 28(e) The contact between the FS and the CS teeth at the end of the engagement

Fig. 28(f) Stress distribution at the end of the engagement

Fig. 29 Variation of contact stresses in the FS and CS

### List of tables

Table 1. Maximum kinematic error for different gear ratios in case of involute profile

# Chapter 1

## Harmonic Drive

### 1.1 Introduction

Reducing the speed or increasing the torque is an important requirement of many power transmission applications. The number of stages required in achieving the above task should be less to obtain high efficiency of the transmission. Many transmission methods are available to reduce the speed which generally needs many stages to achieve high speed ratios. The harmonic drive is a typical transmission device in which large speed reduction is possible in a single stage thus giving high transmission efficiency.

Walt Musser invented the harmonic drive in 1955. Since then it has found widespread use in the field of mechanical engineering. This mechanical transmission also called as 'strain wave gearing' employs a continuous deflection wave along a non-rigid gear to allow gradual engagement of gear teeth. Because of this unconventional gear teeth meshing action, harmonic drives can deliver very high reduction ratios in a very small package. The mechanical operation of this gear drive and the required properties of the components offer new areas of research and analysis. Harmonic drives are particularly suitable for applications where high precision and high transmission ratios are required. These drives mainly consists of three components viz., the wave generator (WG), the flexspline (FS) and the circular spline (CS) as shown in Fig. 1.

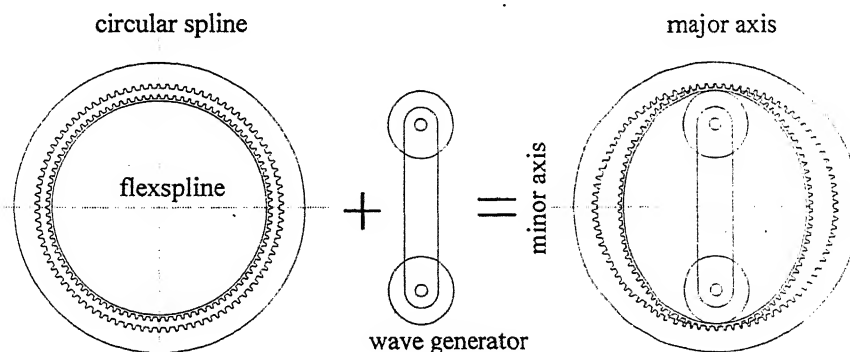


Fig. 1 Harmonic drive

The FS is a thin walled cup adorned with small, external gear teeth around its rim. When assembled, the WG is nested inside the FS, causing the flexible gear to adopt the elliptical shape of the WG. The CS is a rigid gear with internal teeth machined along at slightly large diameter than that of the FS. When the FS and the WG assembly is inserted into the circular spline, the external teeth on the FS mesh with the internal teeth on the CS at two ends of the major axis of an elliptical wave generator.

The main function of the WG is to deflect the FS so that its external teeth engage with the internal teeth of the CS. The WG can be a bar having two rollers at the ends or an elliptical disc. Usually it is connected to the input shaft. In this analysis, a disk type the WG is considered as shown in Fig.2. A flexible roller bearing is used to reduce the frictional loss at the interface of the perimeter of the WG and the inside surface of the cup shaped FS. There exists certain difference in the number of teeth on the FS and the CS. This mismatch in the circular pitches is the reason for obtaining such large speed reduction ratios. When the input rotation is given to the WG, either the FS or the CS should be fixed to obtain the output. If the FS is fixed, its deflection by the WG causes the FS teeth to push the CS teeth. The rotary motion of the WG gives an approximate radial movement to the FS teeth. The action of the FS teeth on the CS teeth results in the rotation of the CS. The speed reduction occurs during the process.

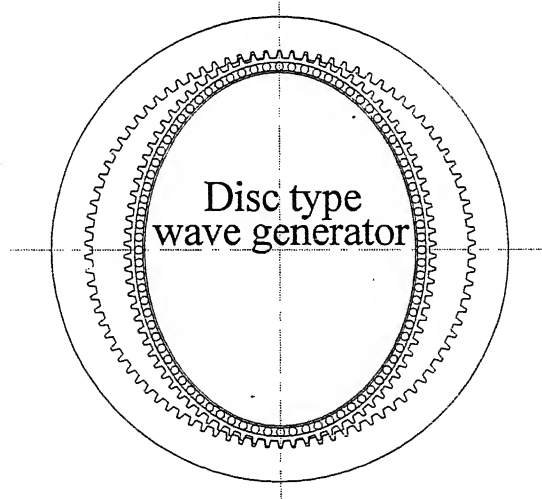


Fig. 2 Harmonic Drive with disc type wave generator



## **1.2 The principle of operation**

As the wave generator rotates, it carries the zone of gear tooth engagement with its major axis. When this zone is propagated  $180^\circ$  around the circumference of the circular spline the FS, which is fixed and contains two fewer teeth than the CS, will rotate the CS by one pitch angle. Through this gradual and continuous engagement of slightly offset gear teeth, every rotation of the WG causes the CS to shift by two teeth.

Through this unconventional gear mechanism, gear ratios up to 320:1 can be achieved in a single transmission [11]. The low torque and high speed input is given to the WG and the high torque and low speed output can be taken either from the FS when the CS is fixed or from the CS when the FS is fixed. Usually the difference in the number of teeth of the FS and the CS is a multiple of the number of contact regions. For maximum transmission ratio this difference is equal to the number of contact regions. In this analysis, the FS is fixed and it has two teeth less than the CS. When the FS is fixed, for one rotation of the WG, the CS rotates by two pitch angles i.e. it shifts by two teeth in the same direction of rotation of the WG.

## **1.3 Performance features and Applicability**

The performance features of the harmonic drive have captured the attention of designers in many fields. The smallest transmissions can provide a maximum torque output of about 3.5 N-m, while the heavy duty units boast up to 10,000 N-m of torque capacity [11]. Gears are available with outer diameters 20 to 330mm with a peak torque capacity from 0.5 to 9000N-m respectively. Because of its unique operating principles, the harmonic drive displays performance features both superior and inferior to conventional gear transmissions.

### **Performance advantages of harmonic drive transmission**

#### **a) High torque capacity**

Because of the multiple-tooth contact, the load is shared by many teeth. Therefore the harmonic drives can transmit high torque.

#### **b) Concentric geometry**

Since all the three harmonic drive components are concentric and coaxial, designers can drastically reduce the power train size and complexity.

c) Lightweight and compact design

Requiring only three basic elements, the harmonic drive can deliver extremely high gear ratios in a small package.

d) Zero backlash

Natural gear preloading and predominantly radial tooth engagement eliminate virtually all transmission backlashes.

e) High efficiency

Properly lubricated harmonic drives can have transmission efficiency from 80 to 90 percent.

### **Performance disadvantages of the harmonic drive**

a) High flexibility

Due to the high loads seen by the wave generator and gear teeth, moderate operating torques can produce substantial transmission torsion.

b) Kinematic error

This error is caused by a number of factors such as tooth placement errors on both the circular spline and flexspline, out of roundness in the three transmission components, and misalignment during assembly.

c) Resonance vibration

Since the torque fluctuations produced by the kinematic error can interact with the low stiffness of the transmission to excite resonances, high vibration amplitudes may be generated in some operating ranges.

d) Non linearity

Both the flexibility and frictional losses in the drive exhibit highly nonlinear behavior.

### **Applications**

Specifically, due to accuracy and simple construction, the harmonic drives have become the choice of designers and engineers in several industries with applications demanding precise positional accuracy and repeatability. The various applications are given below.

#### Machine tools

The precision, repeatability, compactness and high torque to weight ratio of harmonic drive gearing make them a preferred choice of design engineers in the machine tool industry to use in

applications like tool changers. Machines using harmonic drive include routers, milling, water jet cutting, and flame cutting machines.

#### - Robotic applications

Harmonic Drives offer many benefits in robotic applications including zero backlash, high positional accuracy, low vibration and a compact design. They can be used in any of the robot axis and their light weight design contributes minimal weight to the robotic arm which increases robot payload capacity. Hollow shaft harmonic drives allow wiring and vacuum or air lines to connect to external devices through the center of the gear resulting in reducing space requirements.

#### - Medical equipment

Harmonic Drive gears offer zero backlash and high reliability in a compact design to medical equipment designers constantly looking to increase the reliability and decrease the size of their designs. Applications benefiting from harmonic drive gearing include patient beds, rehabilitations equipment. Other uses of harmonic drives include radiation therapy equipment, imaging camera positioning and surgical robots.

Other applications include communication, military surveillance, weather satellites, several deep space probes and telescopes including the Hubble Space Telescope. Harmonic Drives are used to accurately control the antennas and the compass gimbals, to align scientific instruments, adjust apertures and solar panels and to open and close the hatches and doorways.

The main ground based application of harmonic drives are large stationary or truck mounted antennas and arrays used for communications, weapons systems, weather, and civilian and military radar applications. The Harmonic Drives are used to accurately rotate and tilt the antennas and arrays.

Harmonic Drive Reducers are used in these applications because they offer Aerospace and Design Engineers benefits which they cannot find in any other motion control system.

### **1.4 Other mechanisms of speed reduction**

Speed reducers lower motor speed through an increase in torque and a decrease in output speed. They are also known as gear heads or gearboxes which contain a set of gears, input and output shafts. Speed reducer is called a gear head when it is mounted directly onto a motor, not just a

shaft. During equipment operation, the motor transmits power to the input shaft of the reducer. The speed reducer then converts this power into lower output speed, which the reducer transmits to the connected load through the output shaft.

Speed reducers are utilized by a wide variety of industries. Common industries in which reducers are found include the materials handling, automotive, aerospace, construction, food and beverage processing, oil and gas, and textile industries. Reducers are used in a variety of applications, including automation equipment, conveyors, compressors, printing presses, pumps, generators and robotics applications.

The arrangement of the gears in speed reducers is available in many manifestations. Each one is designed for specific load and torque capacities. An example is a cycloidal reducer, which is capable of providing high reduction ratios with high accuracy, with the use of rolling elements. Another formation is that of the planetary reducer, which handles large shock loads well.

Gearheads and other reducers are advantageous in many pieces of equipment. The benefits of using gear heads include speed optimization and performance improvement. When selecting a speed reducer, it is necessary to consider gear ratio, efficiency requirements, and thermal rating.

Generally used speed reducers can be classified as

- a) Worm and worm gear drives
- b) Cycloidal drives
- c) Gearheads

#### **a) Worm and worm gear drive**

This mechanism is used to transmit power through non-intersecting shafts at  $90^\circ$  to each other. The worm is a gear with a single tooth in the form of a screw thread. The worm gear is a special helical gear with teeth formed to avoid interference with the worm. The worm is always used to drive the worm gear; the worm can never be a driven gear in the worm-worm gear pair. The ratio of a worm gear set is the ratio of the number of teeth on the gear to the number of threads (starts or leads) on the worm. For example, a worm with two threads and a mating gear with 60 teeth the drive has a ratio of 30:1.

A worm gear set allows the maximum speed reduction in the smallest package. Worm gear reducers are used in low to moderate horsepower applications. They offer low initial cost, high ratios, and high output torque..

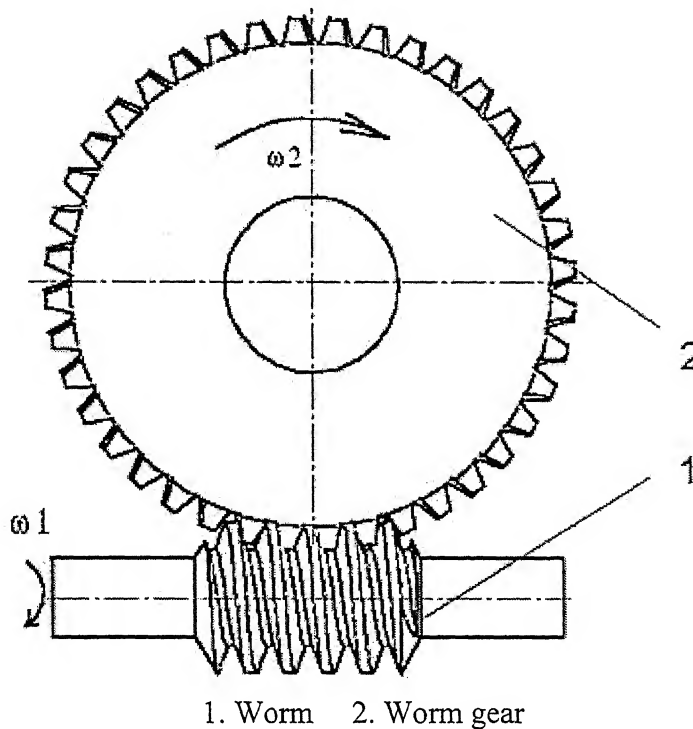


Fig. 3 Worm and worm gear drive

### b) Cycloidal drive

Cycloidal drives transmit power equal to that of gears, but in a smaller and more efficient package. In contrast to the circular motion of gears, cycloidal drives use noncircular or eccentric components to convert input rotation into a cycloidal motion. This cycloidal motion is then converted back into smooth, concentric output rotation. The speed reduction occurs in the process.

#### Principle of operation

The high speed shaft turns the cycloid discs around the internal circumference of the fixed ring gear. With each full turn of the high speed shaft, the cycloid discs advance a distance of one lobe in the opposite direction of the ring gear. The cycloid discs transmit their movement to the slow speed shaft via the slow speed shaft pins. These pins are projected through the cycloid disc bores.

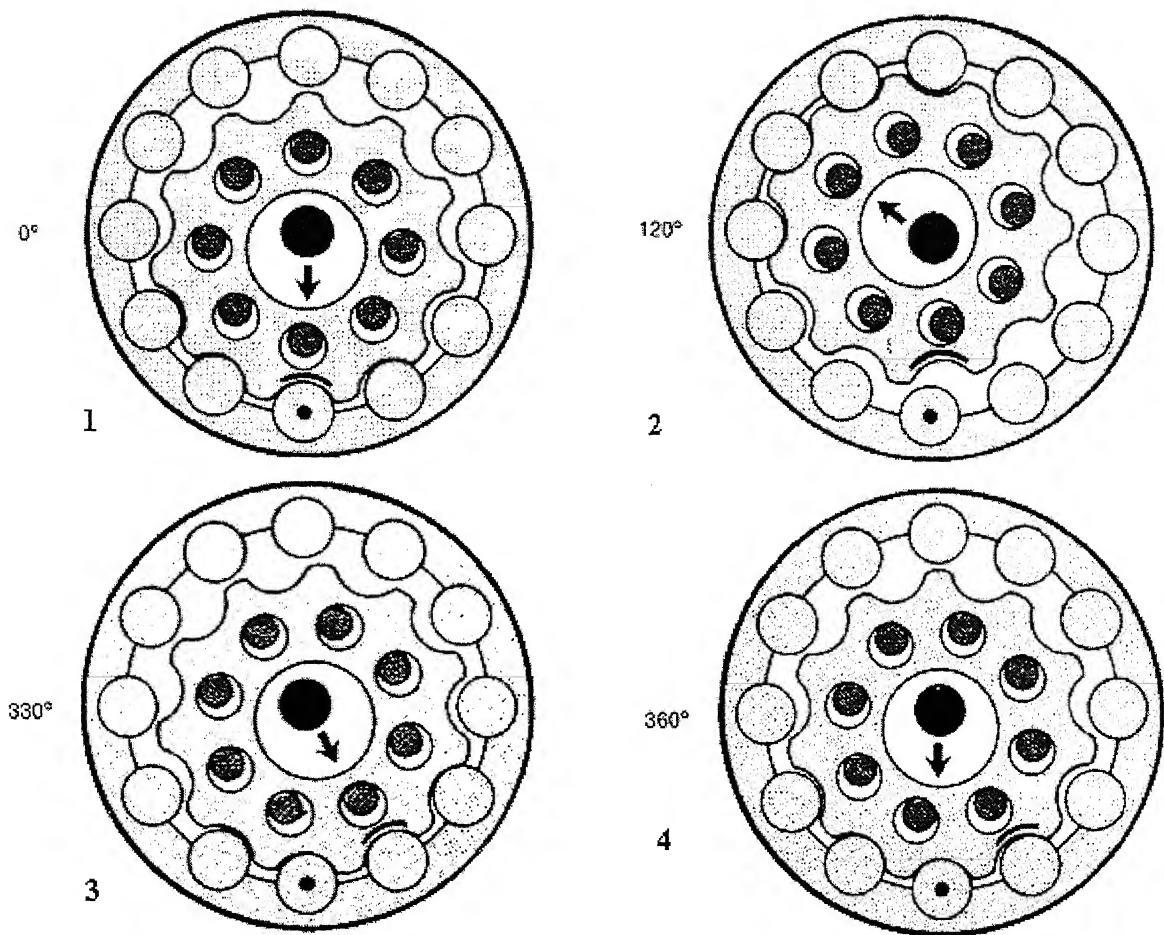


Fig. 4 Cycloidal drive

The term cycloidal is derived from hypocycloidal, which is defined as the curve traced by a point on the circumference of a circle that is rotating inside the circumference of a larger fixed circle. A common example of this motion is the path traced by a tooth of a planetary pinion rotating inside a ring gear.

The worm gearing experiences a dramatic loss of efficiency in going from low to very high input/output speed ratios and the helical gearing loses efficiency at high ratios because two or more stages of reduction are required. The cycloidal drives achieve reduction ratios as high as 120:1 in a single stage, while still maintaining moderately high efficiencies. Moreover, because cycloidal drive components interact in a rolling fashion, failure is generally not catastrophic. As in a bearing, fatigue in the rolling surfaces of a cycloidal drive causes noise levels to gradually increase, serving as a warning long before complete drive failure occurs. Heat generation,

attributed mainly to mechanical losses is readily dissipated through the large surface area of other types of gears. But cycloidal drives, like worm gears, must dissipate heat through a smaller housing surface area. However, because the efficiency of the cycloidal drive is higher than that of the worm gearing of equal capacity and ratio, less amount of heat is generated in cycloidal units. Consequently, the auxiliary cooling often required for worm gear units is usually not needed for cycloidal drives. The concentric shaft orientation also proves valuable, as does the drive's compact size and high reduction capability.

### **c) Gearheads**

The role of a gearhead is closely related to motor development. Originally, when the AC motor was a simple rotating device, the gearhead was mainly used to change the motor speed and as a torque amplifier. With the introduction of motors incorporating speed control functions, the primary role of the gearhead was to amplify torque. But with the wide acceptance of stepping motors and brushless DC motors to meet the requirements for control of speed and position, gearheads found new purposes, including the amplification of torque, improvement in permissible inertia and reduction of motor vibration.

Furthermore, many applications demand for high-precision and backlash-free designs. Gearheads need to be designed with emphasis on high permissible torque, long life, low noise and a wide range of gear ratios. Gearheads for stepping motors are designed for highly accurate positioning, where a high degree of precision, high permissible torque and high speed operation are important. Since servomotors operate most efficiently at much higher speeds than are actually required to drive transducer loads, practically all electromechanical instrument servomechanisms use a reduction gearing between the servomotor and which it actuates. This natural association of servomotor and gearing makes it practical to combine motor and gearhead in a single compact assembly with resultant simplification in servomechanism packaging as well as gains in reliability and cost reduction.

## **Types of gear heads**

### **a) Parallel Shaft Spur Gearing**

Parallel shaft gearheads are the most commonly used gear systems today. The parallel shaft gearheads employ spur gears and helical gears. Helical gears are used for low-noise, high-

strength performance. These are constructed as a train of spur gears, mounted on bearing-supported shafts. But these suffer from the disadvantages like low torque capabilities, high backlash for the frame size and high noise, especially under load. Primary noise contributor is tooth deflection. This gearing requires periodic lubrication.

### **b) Planetary Gearing**

The planetary gear mechanism is comprised mainly of a sun gear, planetary gears and an internal tooth gear. The sun gear is installed on the central axis (in a single stage type, this is the motor shaft) surrounded by planetary gears enclosed in an internal tooth gear centered on the central axis. The revolution of planetary gears is translated into rotation of the output shaft.

As the input sun gear turns, the three planet gears rotate and the load is shared equally across the three planet gears. The planet gear movement is transmitted to the output shaft.

In conventional spur-gear speed reduction mechanisms, gears mesh one to one, so the amount of torque is limited by the strength of each single gear. On the other hand, in the planetary gear speed reduction mechanism, a greater amount of torque can be transmitted, since torque is distributed through dispersion via several planetary gears.

#### Advantages

- High torque output is possible in a small envelope.
- Low backlash.
- High torsional stiffness.
- Load shared equally across three planet gears means longer gear life.
- Self-lubricating gears are maintenance-free.
- All parts rotate concentrically around center axis.

Because today's designs require increasingly higher torque and precision while keeping the package size constant or smaller, most development is being focused upon the planetary gear configuration.



A planetary gearhead should be used over a harmonic/cycloidal drive if the application demands the following characteristics:

#### Constant Velocity and Torque

A planetary gearhead creates speed reduction while maintaining a rolling contact of meshed gear teeth. This allows for extremely smooth motion for both high and low speeds as well as under heavy loads.

#### High Stiffness

A harmonic drive suffers from a lack of stiffness due to the flexspline which is the primary torque carrying member. This lack of stiffness leads to increased lost motion as the load increases which often negate the "zero" backlash feature of this type of drive. The stiffness of a planetary gearhead is determined primarily by the stiffness and number of the hardened steel gear teeth that are in contact at any given time and is therefore extremely high.

#### Low Ratios Under 20:1

Both cycloidal and harmonic drives cannot effectively achieve ratios below 20:1 whereas planetary gearheads with a variety of ratios between 3 and 100:1.

### **1.5 The state of harmonic drive technology**

Throughout its short existence, the harmonic drive has enjoyed continuously increasing international attention from designers as well as researchers. In the Soviet Union, substantial research, predominantly performed on harmonic drives featuring a wave generator with two rollers instead of an elliptical disc, has provided valuable insight into the structural and dynamic properties of the drive as well as its sustainability for heavy duty applications. More recently, Japanese researchers have explored areas of possible research like transmission stiffness, positional accuracy and tooth meshing mechanisms in an effort to develop new gear tooth geometries and improve harmonic drive performance. Investigating the performance of harmonic drive in robotics and aerospace applications researchers in the United States have also contributed constructive insights about the limits of harmonic drive applicability.

Primarily this research has been focused in six major areas:

1. Vibration and dynamic behaviour
2. Kinematic error

3. Torsional stiffness
4. Structural analysis
5. Robotics applications
6. Gear tooth geometry

Much experience has been accumulated in the design of the harmonic drives but their accuracy has not been given much importance.

Istomin and Borisov [1] introduced a method to calculate the kinematic error of the harmonic drive based on the engagement of the FS, noncircular gear, with the rigid round gear. They concluded that the kinematic error of the ideal harmonic drive is on an average 30-40% smaller than the real drive, which is brought about by the errors during manufacturing and assembly. The evaluations of the kinematograms of the harmonic drive which are obtained by experiments establish that as the load increased, the greatest kinematic error decreased.

Emel'yanov et al. [2] proposed an algorithm for determining the influence of the compliances of elements of the harmonic drive transmission on the output kinematic accuracy. The radial compliance of the wave generator unit is determined by the compliance of support bearings of the generator shaft, the bearings of the disc and by the flexural compliance of the shaft. They conducted experiments to determine the radial compliance of the flexible wheel and also the compliance of the engagement.

Popov et al. [3] investigated dynamic stability of drives incorporating harmonic drive transmission by considering the torsional as well as the transverse vibrations. They also proposed a model to calculate the natural frequencies of these vibrations. The relations obtained by them facilitate the detuning of a drive with harmonic drive transmission from resonance which arise from torsional vibrations and transverse vibrations of the transmission, which is particularly important for drives of robotic systems in which natural frequencies of torsional vibrations are located beyond the limits of working speeds of rotation of the wave generators of harmonic drive transmission.

Ivashov and Nekrasov [4] on the basis of fatigue theory of wear derived a formula for determining the theoretical linear wear of teeth of the flexible and rigid wheels of the harmonic drive, depending on the pressure on the contact area, the contact stresses, the coefficient of friction and the modulus of elasticity.

Maiti [5] analyzed the harmonic drive with a new WG cam to drive flex gear of harmonic drives with fully conjugate gear pairs of purely involute profiles without any correction of addendum. The cam profile is composed of circular arcs at the two diametrically opposite contact zones and shifted elliptical curves for other two zones. The geometric construction is done in such a way that the tip interference is properly avoided for both engagement and disengagement with nominally stubbed or full depth tooth involute gears.

Hsia [6] showed that there are inherent positioning errors associated with harmonic drives irrespective of manufacturing and assembly errors. He also showed that errors are very sensitive to the variations in geometric parameters and are functions of angular position of the WG. Kiyosawa, Sasahara and Ishikawa [7] developed a tooth profile to improve durability and stiffness of the strain wave gearing. Kondo and Takada [8] synthesized tooth profiles based to the theory of gear mechanism that the common normal at the meshing point passes through the instantaneous contact point of rolling contact plates (contact point of the WG and the CS pitch curves). Their study on such drives using involute profiles concluded with a proposal for thinner tooth tip to avoid tip interference. But no study on kinematic error is provided.

Gandhi, Ghorbel and Alpeter [9] investigated kinematic error of harmonic drives experimentally. They decomposed the kinematic error into its 'pure' component resulting from the kinematic structure of the harmonic drive and second component due to inherent torsional flexibility. The basic component i.e. the pure kinematic error is obtained by running the harmonic drive at slow speeds to minimize the effect of flexibility. They presented the influence of inertial load, gear assembly and angular velocity on the kinematic error. No design modifications were suggested to reduce the kinematic error.

## **1.6 Kinematic error**

The kinematic error is typically measured by subtracting the rotation at the output of the harmonic drive from the input rotation scaled by the ideal gear ratio for the given transmission configuration. In the drives of high precision machines, more and more extensive use is made of the harmonic gear transmissions having small overall dimensions for a large transmission ratio, a high load carrying capacity and kinematic accuracy. In applications requiring high positional accuracy, the inherent kinematic errors manifested by harmonic drives expose the shortcomings of its transmission.

When designing such drives, it is necessary to reduce the amplitude of kinematic error, which is a source of internal perturbing effects on the drive-over frequencies. Since the harmonic drives are featured by compactness of construction, they can be used effectively in robots and manipulators for which the accuracy in positioning of the executive elements is very important. Therefore, investigations into the kinematic accuracy of the harmonic drives constitute an acute practical problem. Specifically, tooth placement errors on both the CS and the FS, out of roundness in the three transmission components, as well as misalignment during assembly can account for the majority of kinematic imperfections.

Kinematic error though small in magnitude, is periodic in nature and acts as an exciter and hence has an undesirable vibration effects. Since the kinematic inaccuracies in the transmission cause velocity fluctuations, which excite the system resonance, a substantial portion of the operating range of each harmonic drive is contained by serious vibration. These vibrations become dominant at higher speeds, especially at the resonant frequencies. Energy dissipation increases in these regions of resonance and hinders the increase in rotational velocity. An unpredictable jump in velocity can often occur when the transmission harnesses enough energy to push through system resonance.

## **1.7 Objectives**

- To develop a methodology which generates the conjugate tooth profiles for harmonic drives using the condition of constant transmission ratio and maximizing the surface area of tooth contact.
- To investigate the theoretical kinematic error for the harmonic drives with involute teeth profiles. The improvement in the kinematic error for synthesized tooth profile is to be demonstrated and the life of the drive is expected to improve because of the reduced tooth surface wear rate.
- To determine the theoretical mechanical efficiency of harmonic drives with synthesized tooth profiles and compare with that of drives with involute profiles.
- To estimate the contact stress in the circular spline and the flex spline teeth interface using a finite element model and compare the Hertz stress at the teeth contact in the standard involute profiles with that of the synthesized profiles.

# Chapter 2

## Kinematic Analysis and Synthesis

Since the harmonic drive works on the principle of deformable bodies, it is difficult to establish an accurate mathematical model for analyzing the kinematics of the drive. In this work, graphical approach is followed for the kinematic analysis, which gives physical insight into the problem of kinematic error. The WG, usually in an elliptical shape, is connected to the input. The output motion is the result of the relative motion between the CS and the FS. Thus the kinematic error theoretically is a function of the relative motion between the teeth.

### Assumptions in the kinematic analysis

The following assumptions are used in this work:

- The whole system can be treated as a planar mechanism.
- The individual teeth on the FS are rigid.
- Torsional deflection of the FS is negligible.

### 2.1 Path traced by a point on the FS as the WG rotates

For understanding the kinematics of harmonic drives, at first, the path of the FS tooth, during the rotation of the WG needs to be determined. The procedure is explained below.

The initial shape of the FS is circular and assumes the shape of the WG after assembly. The FS is prevented from rotation. Its initial shape is represented by circle  $F$  in Fig. 5. To avoid extra tensile stresses in spite of bending stresses, the circumference of the FS should not be less than the perimeter of the elliptical WG. On the other hand, if the circumference of the FS is greater than the perimeter of the WG, the resulting shape of the FS after being deflected by the WG cannot be found easily since it is a function of material properties.

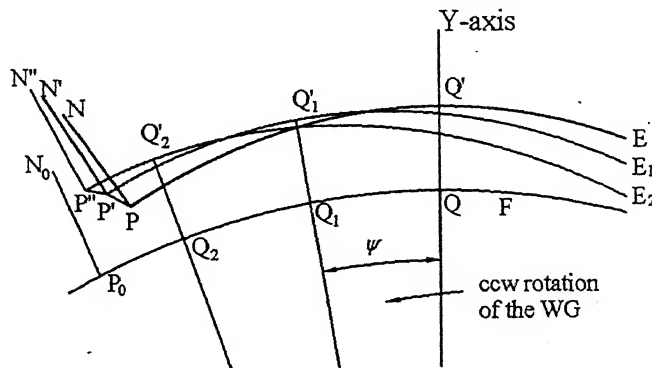


Fig. 5 Motion of a point on the FS

For the purpose of making the analysis simple, the circumference of the FS is taken equal to the perimeter of the WG. Let the center of the tooth base be at point  $P_0$  and the normal to the circle  $F$  at this point is  $P_0N_0$ . This normal is also the axis of symmetry of the tooth. The point  $Q$  is the intersection of the circle  $F$  and the major axis-Y of the WG. When the FS is deformed to an elliptical shape  $E$ , the points  $Q$  and  $P_0$  move to  $Q'$  and  $P$  respectively.

The location of the point  $P$  on an ellipse  $E$  is determined by equating the length of the circular arc  $QP_0$  with that of elliptical arc  $Q'P$ . The next position  $P'$ , the position of  $P$  after a rotation of the WG through an angle  $\psi$  in the counter clockwise direction, is determined by deforming the circle  $F$  to an ellipse  $E_1$  whose major axis is at an angle  $\psi$  in the counter clockwise direction with the Y-axis, and then identifying  $P'$  such that elliptical arc length  $Q_1'P'$  equal to circular arc length  $Q_1P_0$ . Repeating the procedure for all angular positions of the WG the path of the point  $P$  can be traced.

For very small increments in angular displacement of the WG, the motion of the normal can be split into a translation ( $PN \rightarrow P'N_1$ ) and a rotation ( $P'N_1 \rightarrow P'N'$ ) as shown in Fig. 6. The actual point of contact of the FS tooth with the CS tooth is  $P_1$ . Assuming the FS tooth to undergo a rigid body rotation, the final position the point  $P_1$  is given by  $P_1'$ .

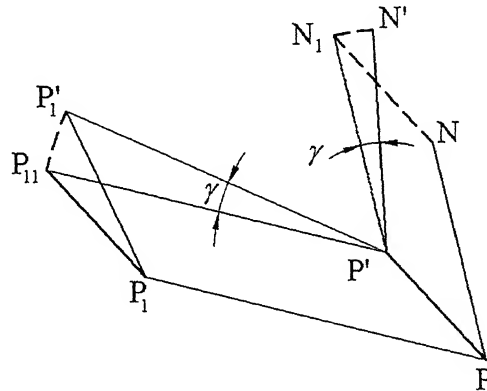


Fig. 6 Change in the direction of normal of the FS tooth

The point  $P_1'$  is obtained by a translation of the line ( $PP_1 \rightarrow P'P_{11}$ ) and then a rotation of  $P_{11}$  about  $P'$  through an angle  $\gamma$ . The path  $PP'$  and the angle of rotation  $\gamma$  are fixed functions of  $\psi$  for the given shape of the WG. The tooth profiles are synthesized considering the motion of the FS tooth imparted by the rotation of the WG and the required motion of the CS. The required motion of the CS (output gear) is determined by the desired transmission ratio, which must remain constant at all instants of time i.e. satisfying the fundamental law of gearing.

## Gear ratio

With the number of teeth of the CS as  $T_{cs}$  and of the FS as  $T_{fs}$ , the angular pitches in an ideal harmonic drive will be

$$\alpha_{cs} = 2\pi / T_{cs} \quad \text{and}$$
$$\alpha_{fs} = 2\pi / T_{fs} \quad (\text{before deflection})$$

The difference  $(\alpha_{cs} - \alpha_{fs})$  is the angle of turn of the driven member of a harmonic drive when the driving member turns through the angular pitch  $\alpha_{fs}$  if the driving (stopped) gear is the FS, or by the angular pitch  $\alpha_{cs}$  if the CS is the driving member. Hence the gear ratio can be expressed as

$$= \alpha_{fs} / (\alpha_{cs} - \alpha_{fs}) = T_{cs} / (T_{cs} - T_{fs})$$
$$= \alpha_{cs} / (\alpha_{cs} - \alpha_{fs}) = - T_{fs} / (T_{cs} - T_{fs})$$

For one revolution of the WG, the CS must be shifted by twice the pitch angle. Therefore, the transmission ratio,  $\rho$  is given by the following relation

$$\rho = \frac{360^\circ}{2 \times \text{pitch angle of circular spline (in degrees)}}$$

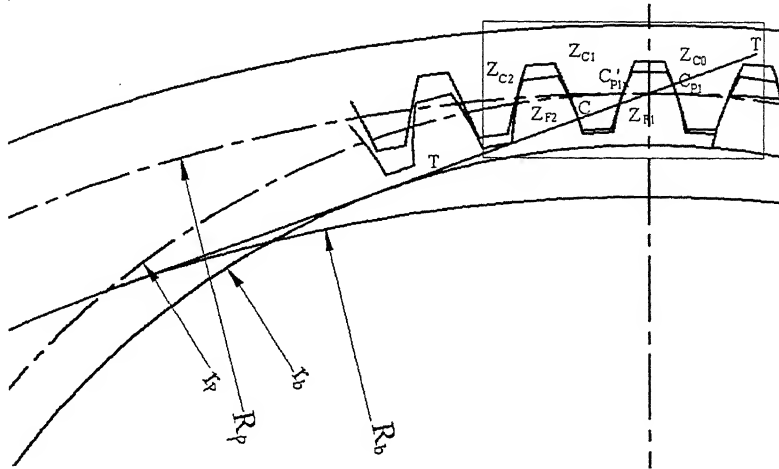
where the pitch angle of the CS is equal to  $360/T_{cs}$ ,  $T_{cs}$  being the number of teeth on the CS. Thus, the transmission ratio,  $\rho = T_{cs}/2$ . So the gear ratio is not a function of size of the gears as in the case of spur and planetary gears. For a rotation of the WG through an angle  $\psi$ , the CS should rotate by an angle  $\psi/\rho$ . The profiles of the FS and the CS teeth must be designed to satisfy this condition for all values of  $\psi$ .

## 2.2 Kinematic analysis of drives with involute profile

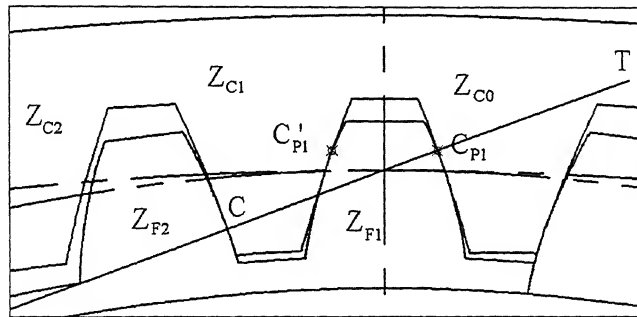
Internal gears produce an output rotation that is in the same direction as the input. Involute spur gears have developed to certain standards and offer a highly effective means of transmitting power. The involute gears with pressure angle  $20^\circ$  are most popular throughout the industry. Simple interaction between the two gears results in a change of speed and torque by the same amount as the ratio of the diameters (or teeth ratio) of the two gears. The power is transmitted through the gear teeth engagements via load sharing across multiple teeth. One of the major advantages of involute gears is their ability to work successfully when the distance between the centres of meshing gears is altered.

The involute tooth profile is used in many harmonic drives. In these cases initially both the CS and the FS are designed as internal gear pair as shown in Fig.7. Let  $Z_{Ci}$  ( $i = 0,1,2$ ) be three

consecutive teeth on the CS,  $Z_{Fi}$  ( $i = 1, 2$ ) be two consecutive teeth on the FS,  $C$  and  $C_{Pi}$  be the contact points of the  $Z_{F2}$  and  $Z_{F1}$  with  $Z_{C1}$  and  $Z_{C0}$ , respectively, and  $C'_{Pi}$  ( $i = 1, 2$ ) be the contact points of  $Z_{Fi}$  ( $i = 1, 2$ ) with  $Z_{Ci}$  ( $i = 1, 2$ ) when  $Z_{Fi}$  are at the apex point of the WG i.e. these are on the major axis of the WG.



(a) Internal gear and pinion



(b) Detailed view

Fig. 7 Internal gear pair

For satisfying the law of gearing, the contact point must always lie on the common tangent ( $TT$ ) to base circles with radii  $R_b$  and  $r_b$  and the both gears to be in circular shape. In the case of a harmonic drive the FS is deformed in shape to a noncircular one; thus the FS tooth  $Z_{F2}$  does not touch  $Z_{C1}$  at the contact point  $C$  as shown in Fig. 8.



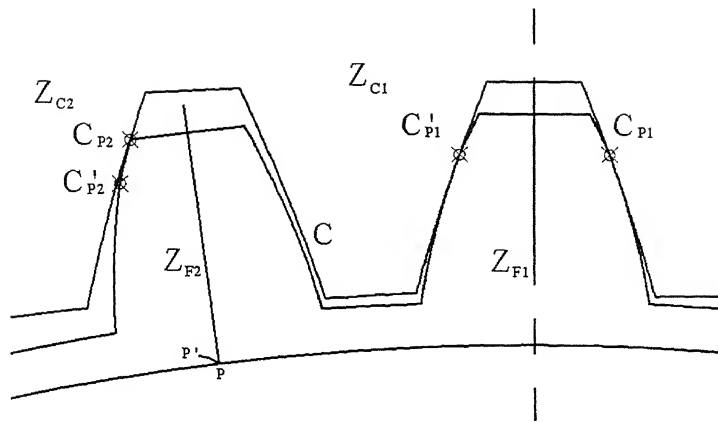


Fig. 8 The contact of the FS teeth with the CS teeth after the FS is deformed.

As the FS changes in shape, the orientation of the tooth  $Z_{F2}$  also changes. To ensure the continuity of motion, it is necessary that the FS and the CS must be in contact all the time. The WG shape should be such that  $Z_{F2}$  touches  $Z_{C2}$  at  $C_{P2}$ .

If the standard addendum is used for the involute teeth, certain tooth portion of  $Z_{F2}$  will definitely interfere with  $Z_{C2}$ . This is because of the small difference in pitch circle diameters of the initial shape of the FS and the CS. To avoid interference, the corrected addendum must be used for the teeth. The amount of correction for the addendum of the FS teeth depends on the dimensions of the elliptical shape of the WG.

### Selecting the dimensions of the WG

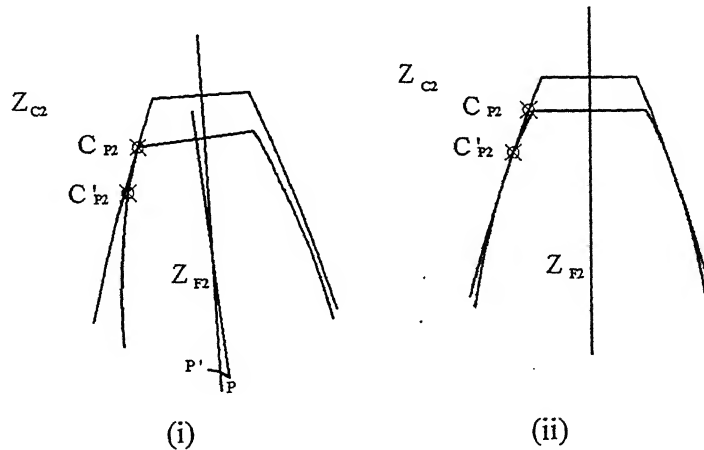
Because the gear ratios fundamentally depend on the number and size of gear teeth, as a rule lower ratios use fewer, larger teeth. Generally, larger teeth require a wave generator with a more elliptical shape to provide sufficient clearance at the minor axis for the teeth to completely disengage. As the flexspline conforms to the rotating ellipse, increasing the wave generator's eccentricity elevates bending and torsional stresses at the base portion of the teeth of the FS resulting in fatigue. Hence it is necessary to have small tooth height. For minimum stresses in the flex spline, it is desirable to keep eccentricity to a minimum.

The dimension of the major axis of the elliptical WG is fixed by considering the internal diameter of the CS and the thickness of the rim of the FS. The dimension of the minor axis should be chosen to avoid the following conditions during assembly of the harmonic drive.

- a) Clearance between the FS tooth  $Z_{F2}$  and the CS tooth  $Z_{C2}$
- b) Interference

These two conditions give two limits for the dimension of the minor axis. But to avoid interference and to maintain contact, the portion of the addendum of the involute teeth should be truncated. However, this truncation should not be below the point  $C'_{P2}$ , which is the contact point of the  $Z_{F2}$  with  $Z_{C2}$  when  $Z_{F2}$  reaches the apex point of the WG. If the truncation exceeds to go beyond  $C'_{P2}$  there will be no contact between the CS and the FS, when position of  $Z_{F2}$  is above the apex of the WG. The value of truncated addendum should again be changed, if the rest of teeth of the FS are interfering with the teeth of the CS.

During the rotation of the WG through one pitch angle of the FS in the counter clockwise direction, the FS tooth  $Z_{F2}$  moves along the path  $PP'$ , thus pushing the CS in the counter clockwise direction. During this motion of the tooth  $Z_{F2}$ , the contact point changes from  $C_{P2}$  to  $C'_{P2}$  as indicated in Fig. 9. So, the contact lengths on the FS tooth and the CS tooth are given by the part of the profiles from  $C'_{P2}$  to the tip of the tooth and  $C_{P2}$  to  $C'_{P2}$ , respectively as shown in Fig. 9.



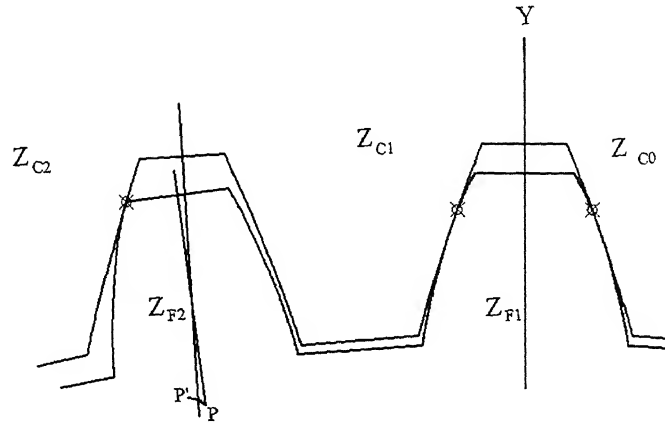
- (i) Beginning of the forward motion of the FS tooth
- (ii) End of the forward motion of the FS tooth

Fig. 9 Forward motion of the FS tooth.

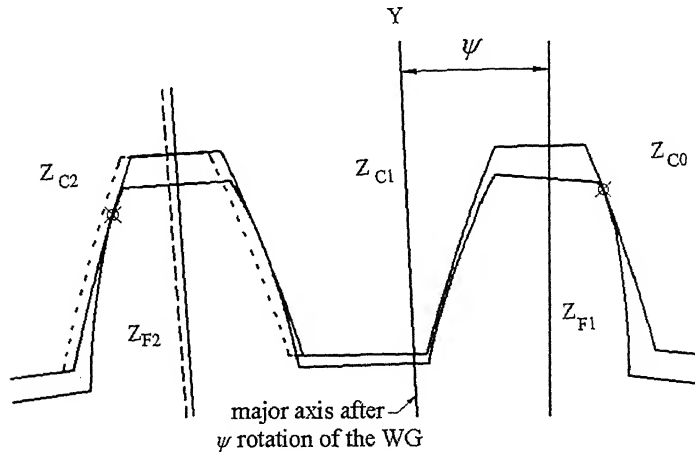
### 2.3 Determination of kinematic error

For a rotation of the WG through an angle  $\psi$ , where  $\psi$  is less than the pitch angle of the FS, the CS may not always rotate by an angle  $\psi/\rho$ . The position of the FS tooth after the rotation of the WG through an angle  $\psi$  is known. The FS tooth is pushing the CS tooth causing the CS to rotate

WG through an angle  $\psi$  is known. The FS tooth is pushing the CS tooth causing the CS to rotate in the counter clockwise direction. Thus the FS tooth is always in contact with the CS tooth. By using this condition, the actual position of the CS can be found. But the ideal position of the CS is obtained by rotating it through an angle  $\psi/\rho$  in the counter clockwise direction. The teeth positions at the beginning and at the end of the rotation of the WG through an angle  $\psi$  are shown in Fig.10 (a) and Fig.10 (b), respectively. The ideal position of the CS tooth is shown in dashed linetype in Fig. 10(b)



(a) Teeth position at the beginning of the rotation of the WG



(b) Teeth position after the rotation of the WG through an angle  $\psi$

Fig. 10 Teeth position before and after finite rotation of the WG

The difference in the ideal and the actual angular positions of the CS, defined as the kinematic error, can be determined. The kinematic error for the rotation of the WG through one pitch angle

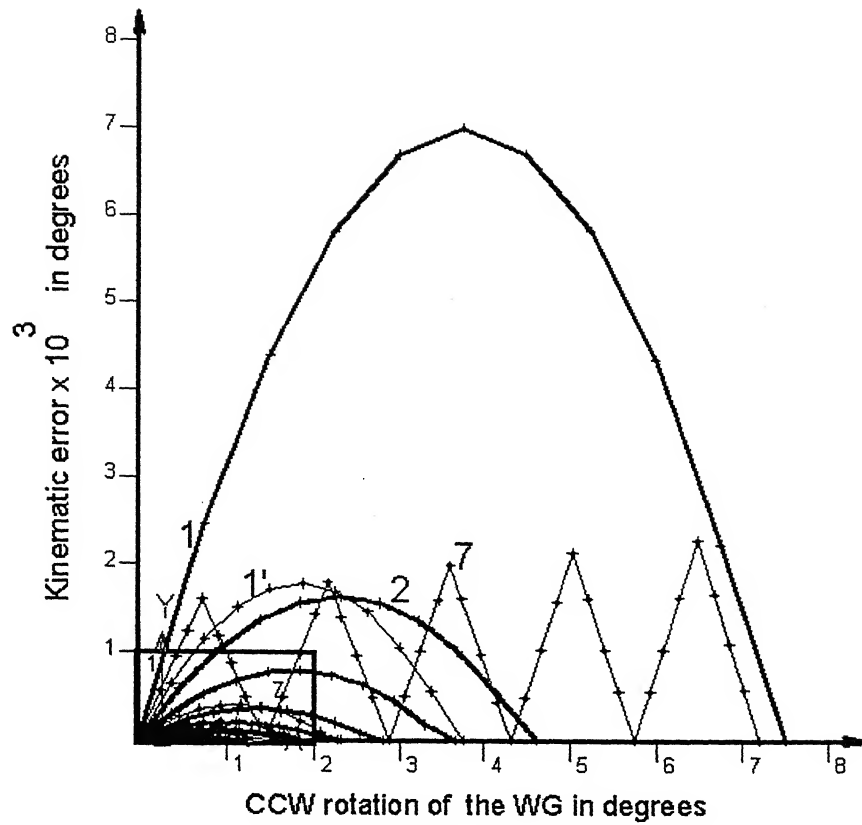


Fig. 11 Kinematic error of Harmonic drives with involute profile for different gear ratios

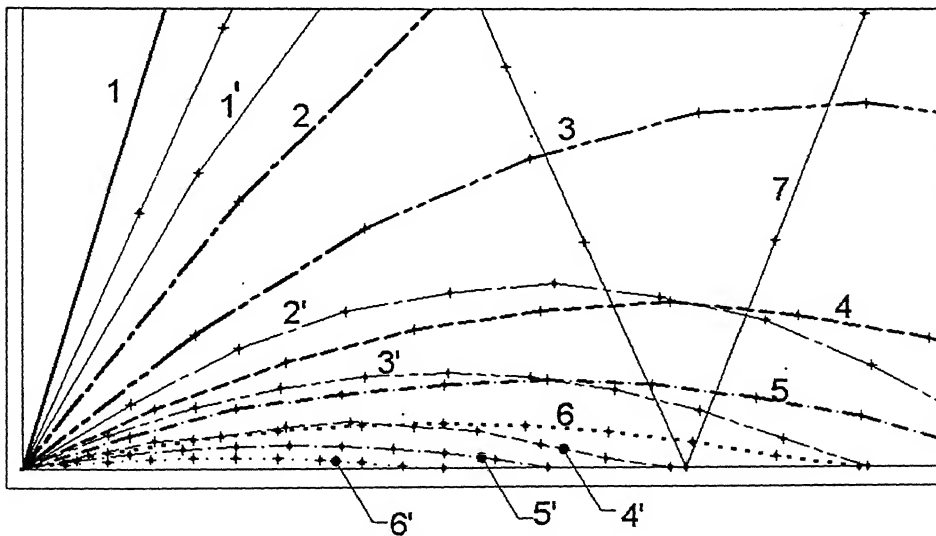


Fig. 12 Detailed view of the kinematic error

Sl. No.	$\rho$	Teeth difference = 2		Sl. No.	Teeth difference = 4	
		Number of teeth, CS/FS	Max. error $\times 10^3$ (in degrees)		Number of teeth, CS/FS	Max. error $\times 10^3$ (in degrees)
1	25	—— 50/48	7.04	1'	—— 100/96	1.79
2	40	--- 80/78	1.63	2'	--- 160/156	0.41
3	50	---- 100/98	0.79	3'	---- 200/196	0.21
4	65	----- 130/128	0.36	4'	----- 260/256	0.10
5	80	----- 160/158	0.19	5'	----- 320/316	0.05
6	100	..... 200/198	0.096	6'	..... 400/396	0.024
7	25	++ 50/48	2.30	SYNTHESIZED PROFILE		

Table 1 Maximum kinematic error for different gear ratios in case of involute profile

The values of the maximum kinematic error for different gear ratios are given in Table 1. It is seen that the kinematic error increases as the gear ratio decreases. Lower transmission ratios are achieved either by decreasing the number of teeth on both the gears or by increasing the difference in the numbers of teeth. For example, the transmission ratio 50:1 is achieved with the CS and the FS having 100 and 98 teeth, respectively. To reduce the transmission ratio to 25:1 either the numbers of teeth on the CS and the FS can be reduced to 50 and 48, respectively or by keeping the number of teeth on the CS as 100 and reducing the number of teeth on the FS to 96. The kinematic error for synthesized tooth profile is found by approximating the profile with 5 segments. If more segments are taken, the kinematic error can further be reduced.

## 2.4 Synthesis of tooth profiles

It is already mentioned that the kinematic error is a function of relative motion between the FS and the CS teeth. The objective of this work is not only to reduce the kinematic error but also to maintain the geometry of the teeth profiles. If the rate of wear on the profiles is less, then they can retain their shape for a longer working period. During the relative motion between the teeth of the FS and the CS, the point of contact continuously changes on both the profiles.

Let the profile length  $l$  be in contact during the time period  $t$ , which is the time interval between the engagement and the disengagement of the teeth of the FS and the CS. If the value of  $l$  is

increased, for the same time period  $t$ , the depth of wear is less on any of the profiles. This will result in maintaining the geometry of the profiles for a longer time.

Figure 13 shows two circles  $A$  and  $B$ , which are always in contact. Let the circle  $A$  be constrained to move in the direction indicated by an arrow and the circle  $B$  moves such that its center shifts from  $O_1$  to  $O_2$  as shown in the figure. The points  $O_{1A}$  and  $O_{2A}$  indicate the center of the circle  $A$  before and after its movement, respectively.

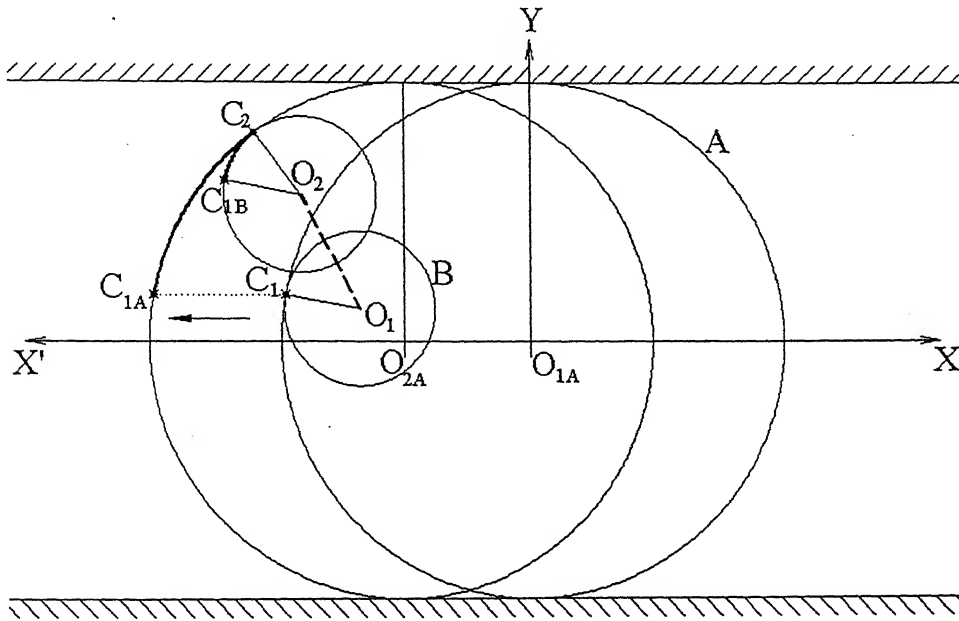


Fig. 13 Displacement of circle  $A$  and circle  $B$

The initial and the final contact points of the circles  $A$  and  $B$  are  $C_1$  and  $C_2$ , respectively. The lengths of the arcs of contact are  $C_{1A}C_2$  and  $C_{1B}C_2$  on circles  $A$  and  $B$ , respectively. Since the arc length  $C_{1A}C_2$  is greater than the arc length  $C_{1B}C_2$  there exists a certain amount of sliding of the circle  $B$  on the circle  $A$ . The movement of the circle  $A$  and the path followed by the center of the circle  $B$  satisfy a definite relationship. When the motions are prescribed, the profiles of the two bodies always maintaining contact can be synthesized.

Let the body  $A$  be the CS and the body  $B$  be the FS. The part of the profiles in contact of the CS and the FS teeth are assumed as straight lines during a small rotation of the WG. At the beginning, the FS and the CS teeth profile segments,  $SF$  and  $SC$ , are at an angle  $\theta$  with the line

$X_1X_2$ , which is the tangent to an imaginary circle concentric to the CS and passing through the point of contact  $P_1$ , as shown in Fig.14. The angle made by a small segment of the path  $P_1P_1'$  with the tangent  $X_1X_2$  is represented by  $\phi$ .

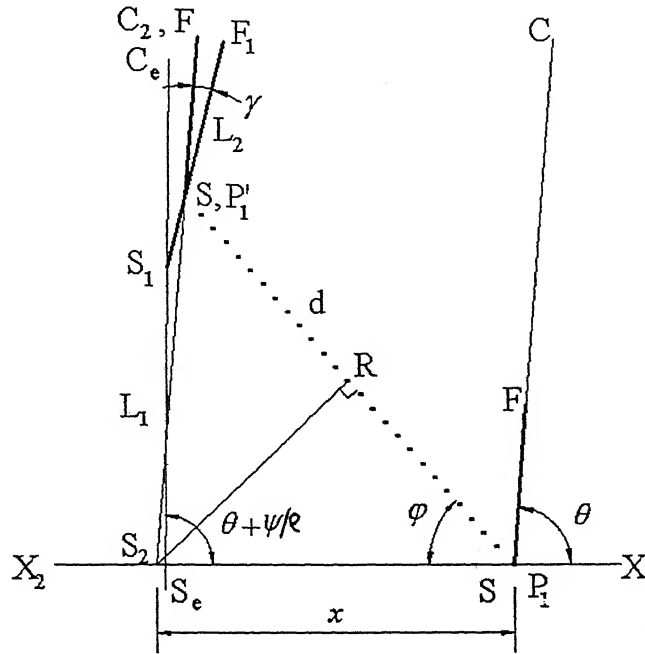


Fig. 14 Approximate motion of the CS for the given motion the FS teeth

Let  $x$  be the small displacement of the CS tooth due to small rotation  $\psi$  of the WG. Thus,

$$x = \pi r \psi / (180\rho)$$

where the rotation of the wave generator  $\psi$  is in degrees and  $r$  is the distance of the contact point from the center of the CS. The displacement of the FS tooth during the rotation of the WG through an angle  $\psi$  is given by  $d$ . This is a function of rotation of the WG and its shape. Considering only the translation of the FS segment for a small rotation of the WG, the required angle  $\theta$  can be determined. From the geometry shown in Fig. 14,

$$d = P_1R + RP_1' = x \cos \phi + x \sin \phi \tan (\theta - (90 - \phi))$$

$$\tan(\theta + \phi) = x \sin \phi / (x \cos \phi - d) \quad (1)$$

The value of  $\theta$  less than  $90^\circ$  is determined for the given values of  $d$ ,  $x$  and  $\phi$ . To avoid the interference of the FS tooth with the CS tooth due to change in orientation of the FS tooth, the value of  $\theta$  at any instant should be less than  $90^\circ$ . Therefore, the limiting value of  $d$  is  $x/\cos \phi$ .

The value of  $\theta$  should be as large as possible to reduce the radial component of the force at the contact point of the teeth. If the shape of the WG is ellipse, then the value of  $d$ , the displacement of the FS tooth for a rotation of WG through an angle  $\psi$ , may be more than  $x/\cos \varphi$ . Therefore for rotating the CS by an angle  $\psi/\rho$ , with the elliptical WG, the value of  $\theta$  cannot be less than  $90^\circ$ . To limit the value of  $\theta$  less than  $90^\circ$ , either the value of  $d$  should be reduced or the value of  $\varphi$  should be increased. Increasing the eccentricity of the WG can increase the value of  $\varphi$ . High value of eccentricity of the WG leads to more bending stresses in the FS.

Since the shape of the WG to avoid interference is not known initially, the elliptical shape can be taken as initial approximation. By changing the value of  $d$ , the path of the FS tooth changes. There exists a unique path of the FS tooth for the given shape of the WG. Therefore the shape of the WG can be determined for the modified path of the FS tooth. The value of  $d$  should be adjusted such that the value of  $\theta$  measured with line  $X_1X_2$  goes on decreasing from the starting of the motion of the FS tooth to the end of its motion i.e. till it reaches the apex position of the WG.

Initially, the FS and the CS teeth segments are in contact as shown in Fig. 14. During the motion of the FS tooth, the segment  $SF$  pushes the CS segment  $SC$  towards left, which causes the CS to rotate in the counter clockwise direction (in the direction of the rotation of the WG). The final positions of the FS and CS segments are shown by  $SF_1$  (obtained after change in orientation of the FS tooth by an angle  $\gamma$ ) and  $S_2C_2$ , respectively. But, the ideal position of the CS after the rotation through an angle  $\psi/\rho$  is given by  $S_eC_e$  which makes an angle  $\theta + \psi/\rho$  with the line  $X_1X_2$ . To move the CS to the ideal position, the FS segment is extended backwards to meet  $S_eC_e$ . The FS segment length  $SF$  must always be less than the segment length  $S_eS_1$  to have proper initial contact.

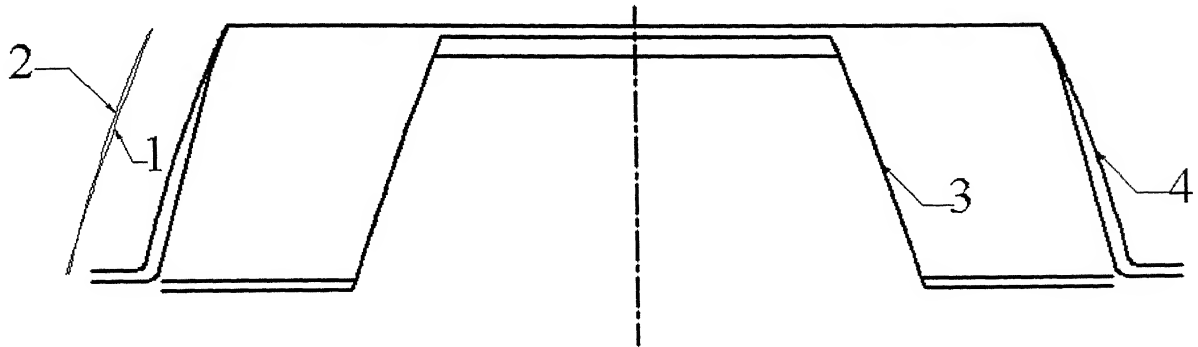
The value of  $\theta$  can be slightly adjusted to have more length of the FS segment. This leads to increase in the length of contact on the part of FS tooth profile. As more length of the FS tooth profile is involved in contact action during the rotation of the WG, the depth of wear on the profile is less, which helps in maintaining the shape of the profiles for a long time and thus increasing the reliability of the drive with respect to kinematic accuracy. The part of the profiles of the FS and the CS are the segments  $SF_1$  and  $S_eS_1F_1$ , respectively. The CS tooth profile



segments  $S_eS_1$  and  $S_1F_1$  are represented by  $L_1$  and  $L_2$ , respectively. Now, the point  $F_1$  can be taken as point  $P_1$  and find the next value of slope of the profile corresponding to next segment of the path. By repeating this procedure, the teeth profiles of both the FS and the CS can be obtained.

## 2.5 Comparison between the involute and the synthesized tooth profiles

Figure 15 shows the synthesized and the involute profiles when the axis of symmetry of the teeth is aligned with major axis of the WG.



1. Involute profile 2. Synthesized profile 3. Involute pair 4. Synthesized pair

Fig. 15 The synthesized and the involute tooth profiles

Even though the involute profiles of the CS and the FS are looking same, but there exists a small difference. This is due to the small difference in the diameters of the base circles of the pinion and the internal gear. The synthesized profile depends on the FS tooth motion, which in turn is a function of the shape of the WG. Thus, for any modified shape of the WG, there exists a unique profile that gives no kinematic error. In case of synthesized profiles, the point of contact is from starting to the ending of the teeth profiles. This is similar to the lengths of contact of the circles shown in Fig. 13.

### Synthesis procedure when the shape of the WG is an ellipse

Since the value of  $d$  is high for elliptical WG, the value of  $\theta$  is more than  $90^\circ$ . The synthesis can slightly be modified to obtain a reasonable shape of the teeth.

At the beginning, the FS and the CS teeth profile segments  $SF$  and  $SC$  are at an angle  $\theta$  with the line  $X_1X_2$ , which is the tangent to an imaginary circle concentric to the CS and passing through

the point of contact  $P_1$ , as shown in Fig.16a. The angle made by the path  $P_1P_1'$  with the tangent  $X_1X_2$  is represented by  $\phi$ .

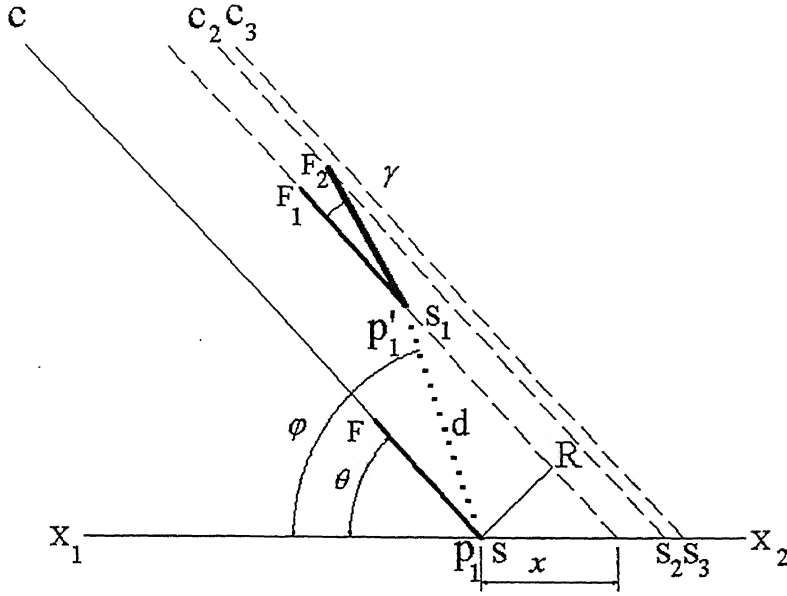


Fig. 16a. Approximate motion of the CS for the given motion the FS teeth

During the motion of the FS tooth, the segment  $SF$  pushes the CS segment  $SC$  towards right, which causes the CS to rotate in the clockwise direction (opposite to the rotation of the WG). Let  $x$  be the small displacement of the CS tooth due to small rotation  $\psi$  of the WG. Thus,

$$x = \pi r \psi / (180\rho)$$

where the rotation of the wave generator  $\psi$  is in degrees and  $r$  is the distance of the contact point from the center of the CS. Considering only the translation of the FS segment, the required angle  $\theta$  can be determined. From the geometry shown in Fig. 16a,

$$P_1R = x \sin \theta = d \cos (180 - \phi - (90 - \theta)) = d \sin (\phi - \theta)$$

$$d = (x \sin \theta) / \sin (\phi - \theta) \quad (2)$$

So, there exists a value of  $\theta$  less than  $90^\circ$  for the given values of  $d$ ,  $x$  and  $\phi$ . Due to change in the orientation of the FS tooth, the direction of the segment  $S_1F_1$  changes to  $S_1F_2$ . This change in angle is equal to the rotation of the normal  $\gamma$  as shown in Fig.6. This makes the CS to rotate in the clockwise direction to  $S_2C_2$  as indicated in Fig. 16. The ideal position  $S_3C_3$  of the CS is determined based on the required angle of rotation  $\psi/\rho$ . To rotate the CS to the ideal position, the

FS segment  $S_1F_2$  can be extended to meet the CS segment  $S_3C_3$  at point  $F_3$  as shown in Fig. 16b. The required lengths of the CS and the FS segments are given by  $S_3F_3$  and  $S_1F_3$ , respectively. The point  $F_3$  is taken as the point  $P_1$  and by repeating the procedure for the whole motion of the FS tooth, the teeth profiles of the FS and the CS are obtained. The segment  $S_3F_3$  of the CS is represented by  $L_1$ .

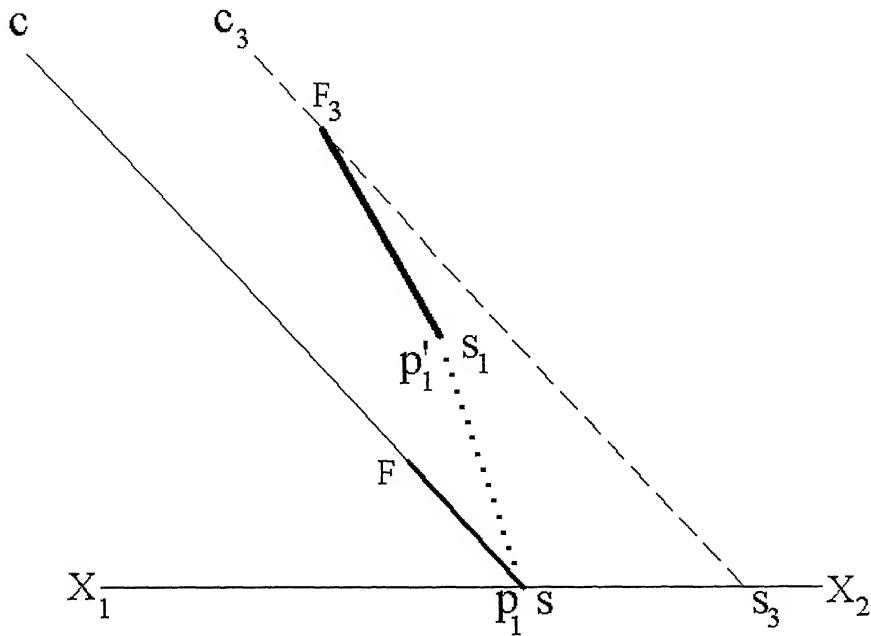
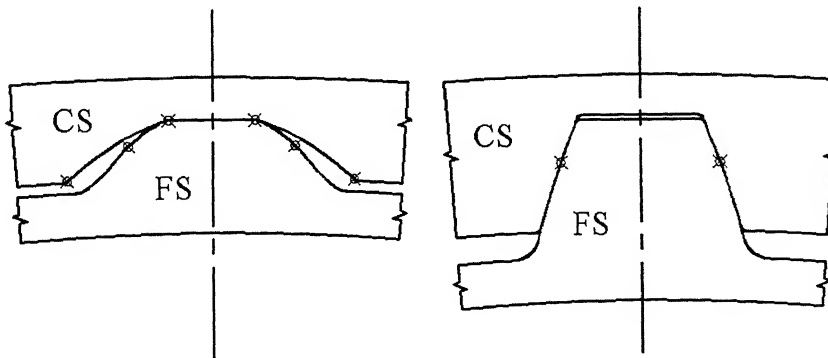


Fig. 16b The final segments after extending the FS segment to meet the CS segment

#### Comparison between the involute and the synthesized profiles



(i) Synthesized

(ii) Involute

Fig. 17 The synthesized and the involute tooth profiles

The synthesized and the involute profiles are shown in Fig.17. The pressure angle for the synthesized profile is higher than that of involute profile. This increases the magnitude of the radial component of the contact force. Due to high contact force, the magnitude of stresses generated in teeth will be high. In addition to this, since the value of coefficient of friction increases with the increase in magnitude of contact force which ultimately leads to more power loss.

### Possible number of teeth in contact

The contact ratio can be increased till the total length  $L = L_1 + L_2 + L_3 + \dots$  of the CS teeth profile given by the sum of the all segment lengths, cover an angle equal to  $180^\circ/T_{cs} - \beta_1 - \beta_2$  as shown in Fig. 18.  $\beta_1$  and  $\beta_2$  are the angles covered by the half of the bottom and top lands of the CS teeth respectively.

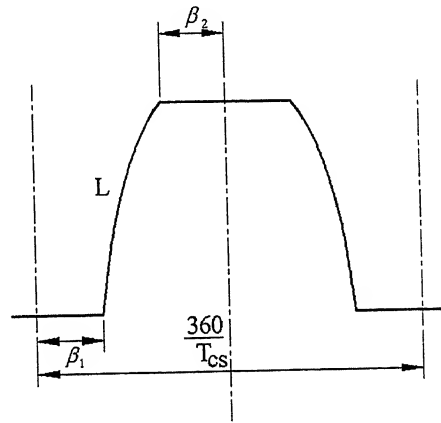


Fig. 18 Circular spline teeth

# Chapter 3

## Mechanical Efficiency

The efficiency serves as one of the principal characteristics by which a particular type of reduction gear is chosen. The value of efficiency is needed

- a) for assessing the energy consumption of the drive,
- b) for calculating the power of the drive motor and
- c) for the selection of methods of cooling

The power loss in a pair of gear of any kind mainly consists of sliding friction between the teeth surfaces. The conditions of tooth engagement in respect of the intensity of pressure and the sliding and rolling velocities vary from instant to instant. The instantaneous coefficient of friction will likewise vary, and since present knowledge of the coefficient of friction under such varying conditions is not perfect, the calculation of gear tooth efficiency on theoretical grounds is only approximate.

### Factors influencing the coefficient of friction

All harmonic drives exhibit power loss during operation due to friction. The combination of friction with gear compliance renders it difficult to achieve high precision speed, position and torque control in pointing and tracking servomechanisms. The coefficient of friction is the principal source of inaccuracy in calculation. It depends upon the materials, the surface finish of the teeth, sliding velocity, and the type of lubricant. These factors can be investigated only by experiments.

### 3.1 Theoretical determination of mechanical efficiency

Let  $N_1N_1$  and  $T_1T_1$  be the normal and tangent to the teeth profiles at the contact point, respectively as shown in Fig. 19. The applied output torque  $T_{out}$  is equal to the product of  $P_0$  and the radius  $r$ , which is equal to the distance between the contact point and the center point of the CS. The normal component of the force  $P_0$  is equal to  $P_n$ , which is given by  $P_0 \sin \theta$ .

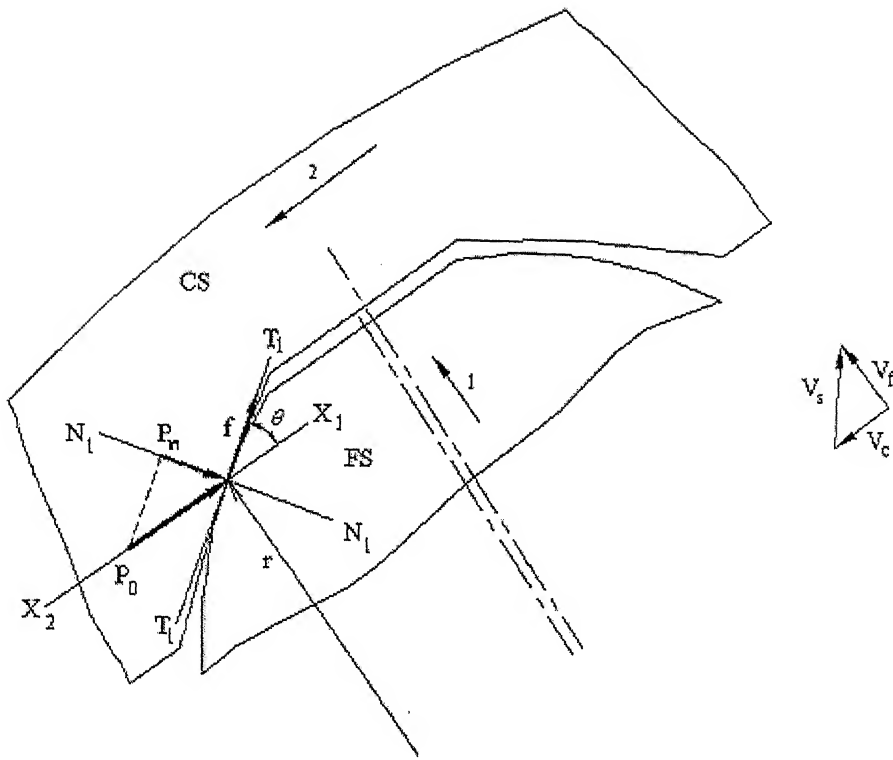


Fig. 19 Forces acting at the interface of the teeth contact

The direction of movement of the FS tooth during the rotation of the WG is indicated by arrow 1. The pushing action of the FS tooth on the CS tooth causes the CS to move in the direction shown by arrow 2. In this configuration, the frictional force acting on the CS at the interface is represented by  $f$ .

When a body is sliding on another body the coefficient of friction is mainly a function of sliding velocity. The variation of the coefficient of friction with sliding velocity between the teeth of the harmonic drive is still unknown. From numerous tests of complete worm reduction gear units over a wide range of conditions of load, speed, and detail design the experimental results for the variation of coefficient of friction with sliding velocity were well established [10]. As a better approximation, these results are used in the case of the harmonic drive. The relation between the friction coefficient and sliding velocity in the case of worm gear drive is given by

$$\mu = \frac{0.2}{e^{0.17\sqrt{V_s}}} + 0.0013\sqrt{V_s} \quad (3)$$

In this relation the velocity should be substituted in ft/min to obtain the value of the coefficient of friction. Figure 20 shows the variation of coefficient of friction by taking the velocity in m/s.

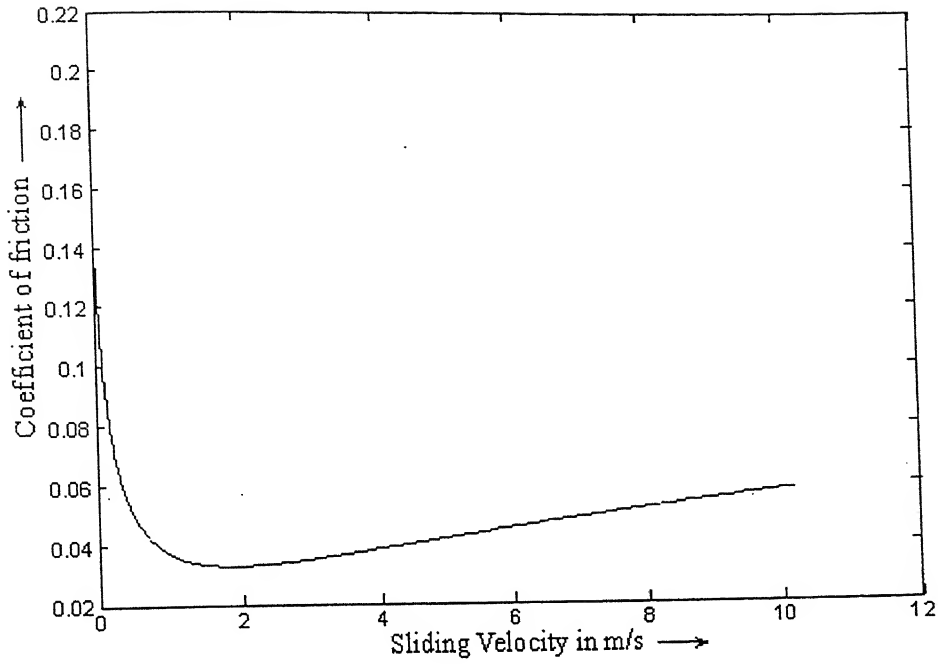


Fig. 20 Variation of coefficient of friction with sliding velocity

Total power loss in the harmonic drive from input to the output can be divided mainly into four parts given below:

- Power loss in the ball bearing at the input shaft
- Loss of power due to flexible roller bearing between the wave generator and the flexspline
- Power loss due to friction at the interface of the teeth profiles of the CS and the FS
- Power loss in the ball bearing at the output shaft

In this analysis for the purpose of calculating the mechanical efficiency only the losses occurring at the interface of teeth is considered. The energy loss due to friction between the teeth profiles is

given by

$$P_f = \int_{t_1}^{t_2} \mu P_n V_s dt \quad (3)$$

where the time between the starting of the engagement of the teeth to the disengagement is represented by the interval from  $t_1$  to  $t_2$ . The normal load and the sliding velocity are functions of time and the coefficient of friction is a function of sliding velocity. Now, the power lost at the interface of the tooth profiles in the harmonic drive can approximately be estimated from the expression (3). The efficiency can thus be calculated for the applied output torque and the given

input speed. Since the power at the output shaft and the losses are known, the input can be equated to the sum of the output power and the losses.

$$\eta = \frac{\text{output}}{\text{output} + \text{losses}}$$

In the normal cases, the coefficient of friction does depend upon both the normal load and the sliding velocity. But the effect of normal load on the coefficient to friction is less dominant than the sliding velocity. Therefore the variation of coefficient of friction due to change in normal load is neglected in this analysis.

### 3.2 Effect of speed on mechanical efficiency

Figure 21 shows the relation between efficiency with the input speed. Since the bearing losses are not considered the mechanical efficiency seems high. The efficiency graphs are shown for speed ratio 25. At very high speeds, the losses increase due to increase in the coefficient of friction. Therefore the mechanical efficiency decreases with the increase in speed.

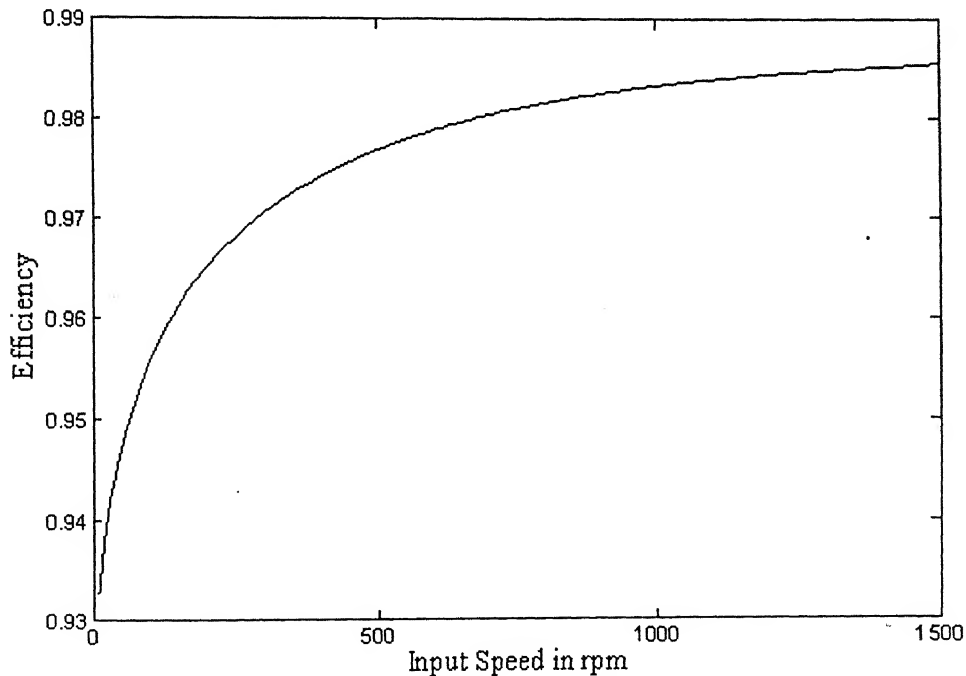


Fig. 21(a) Variation of efficiency with the input speed for gear ratio 25 (over a short range)



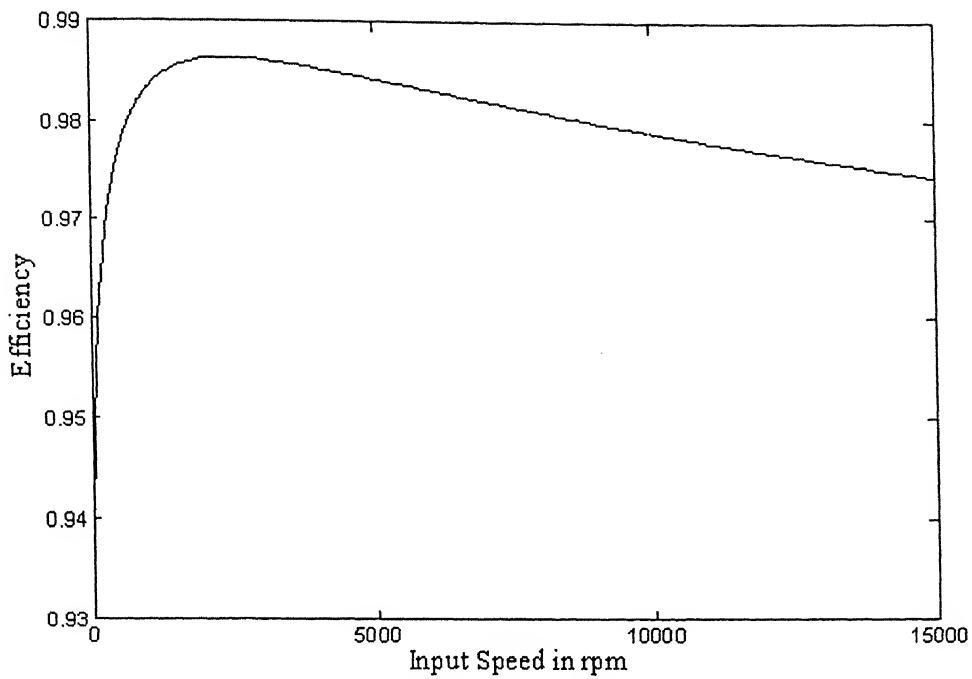


Fig. 21(b) Variation of efficiency with the input speed for gear ratio 25 (over a large range)

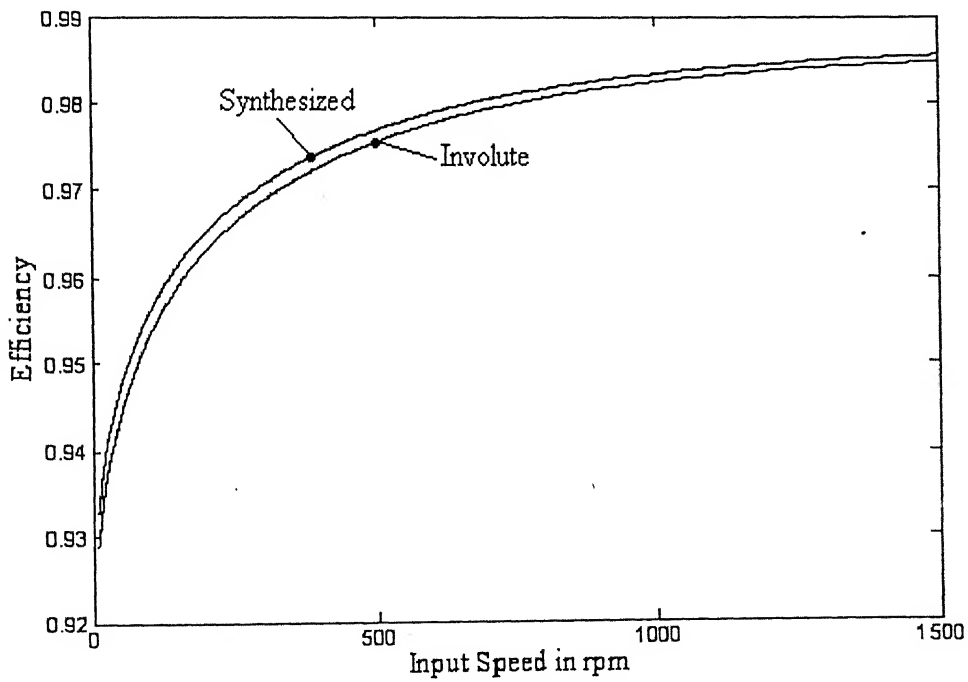


Fig. 21(c) Mechanical efficiency of drive with involute and synthesized profiles (gear ratio 25)

In the case of synthesized profiles, as more number of teeth are in contact, the load acting on one tooth is less. On the other hand, in the harmonic drives with involute teeth profiles, the number of teeth in contact is less. Since the losses increases with the increase in load, the efficiency of the harmonic drives with synthesized profiles is high compared to those with involute profile as shown in Fig. 21(c).

As the output resisting torque increases, the normal load acting on the teeth profiles increases. The effect of this can reflect in increase in the coefficient of friction, which increases the magnitude of the power lost. This effect finally manifests in decrease in efficiency of the drive. The value of the coefficient of friction with increase in load is assumed slightly higher. The variation of mechanical efficiency with the increase in torque is approximately shown in Fig. 22.

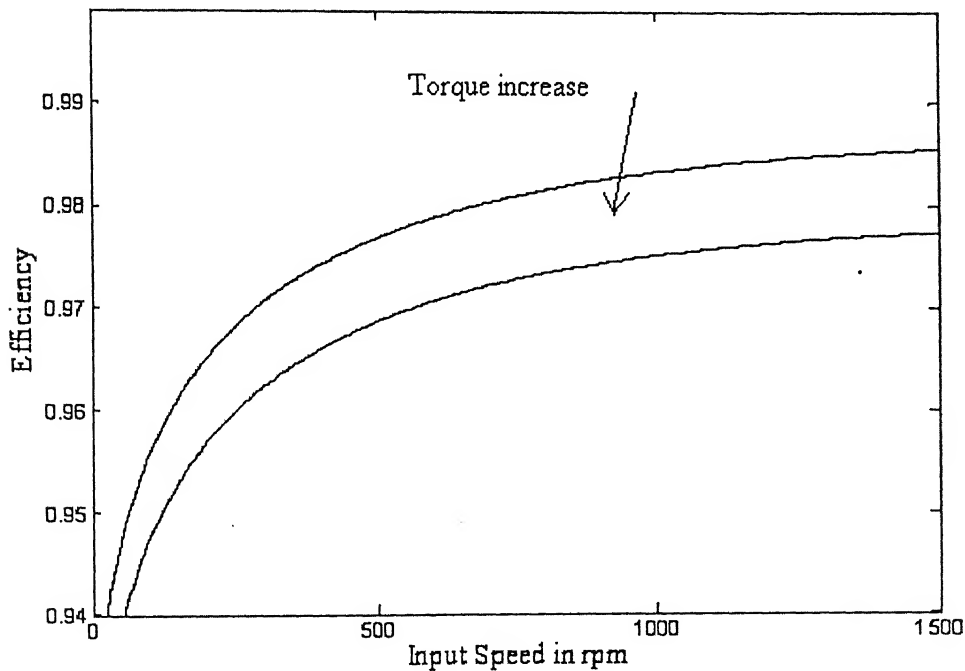


Fig. 22 Variation of efficiency with increase in torque for gear ratio 25 (over a large range)

### 3.3 Effect of gear ratio on mechanical efficiency

To increase the speed ratio, it is necessary to increase the number of teeth on the CS and the FS. As the number of teeth increases, their position of teeth in contact is close to the apex of the WG. So, they move only small distance corresponding to the rotation of the WG. Therefore the sliding velocity of the FS teeth on the CS teeth decreases. In the operating speed range (500-2000 rpm) this leads to increase in friction. So the mechanical efficiency decreases. The velocity profiles for speed ratio 25 and 100 are shown in Fig. 25(b) and Fig. 26(a) respectively. The operating velocities are in the range where the coefficient friction has negative slope. Figure 23 shows the effect of gear ratio on the efficiency.

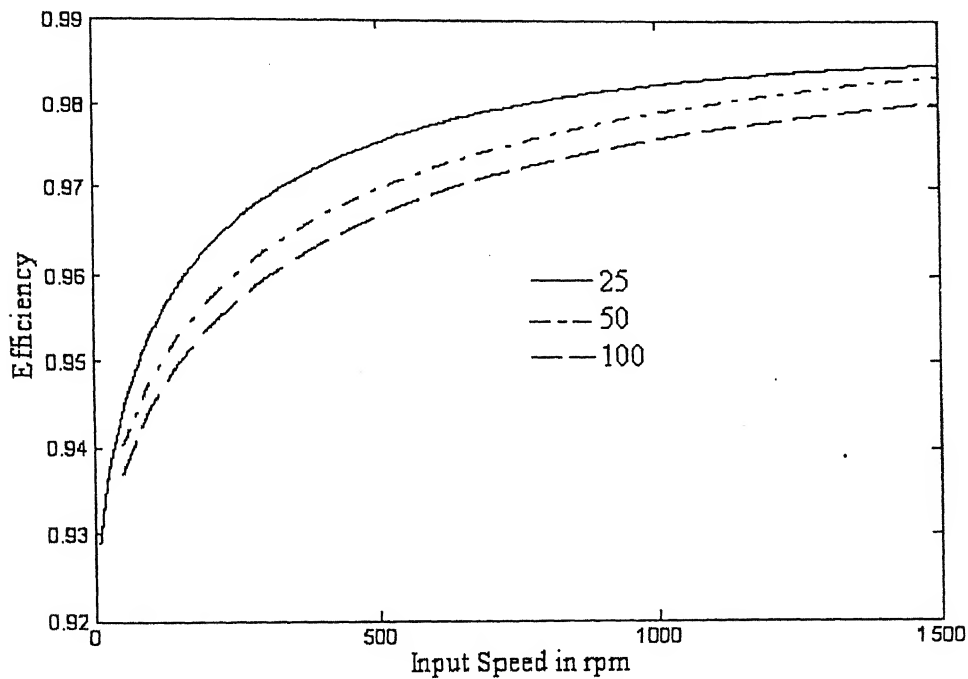


Fig. 23 Mechanical efficiency with different speed ratio (involute profile)

### 3.4 The velocity profile of the FS tooth

The variation of velocity of the FS tooth from the start to the end of the engagement for the modified WG shape is given below. These graphs are shown for different speeds of the WG. In case of synthesized profiles as the number of teeth in contact is higher, the velocity of the FS tooth whose position is considerably away from major axis is shown in Fig. 24. The velocity profile for the 4<sup>th</sup> teeth counting in the counterclockwise direction from the major axis is given in the graph for the gear ratio 25. Where as in the harmonic drives with involute teeth, the number of the FS teeth in contact with the CS teeth is less (to avoid interference). Therefore the velocity profiles are shown for the first teeth counting in the counterclockwise direction from the major axis. The radial distance travelled by the teeth increases as its position goes away from the major axis. Therefore the velocities in the drives with involute profiles are lower compared to that of the drives with synthesized profiles. In the case of involute teeth as the gear ratio increases, the first tooth of the FS comes closer to the major axis. This results in further reducing the velocity of the FS tooth.

#### Velocity profile in the case of synthesized profiles

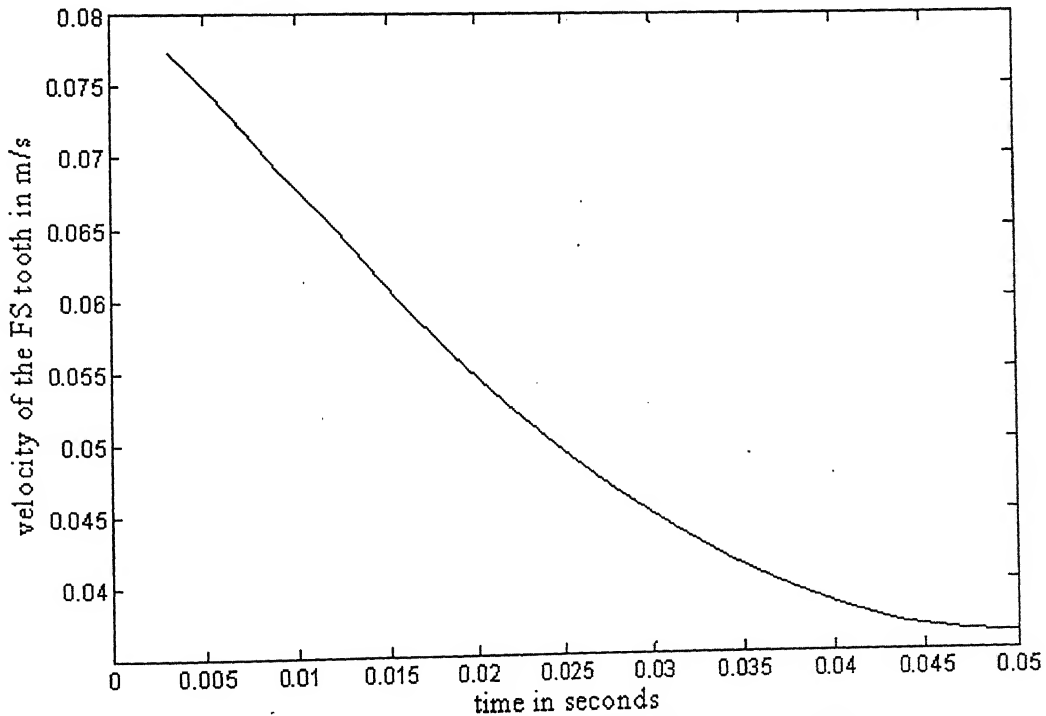


Fig. 24(a) Velocity of the FS tooth at the input speed 100 rpm

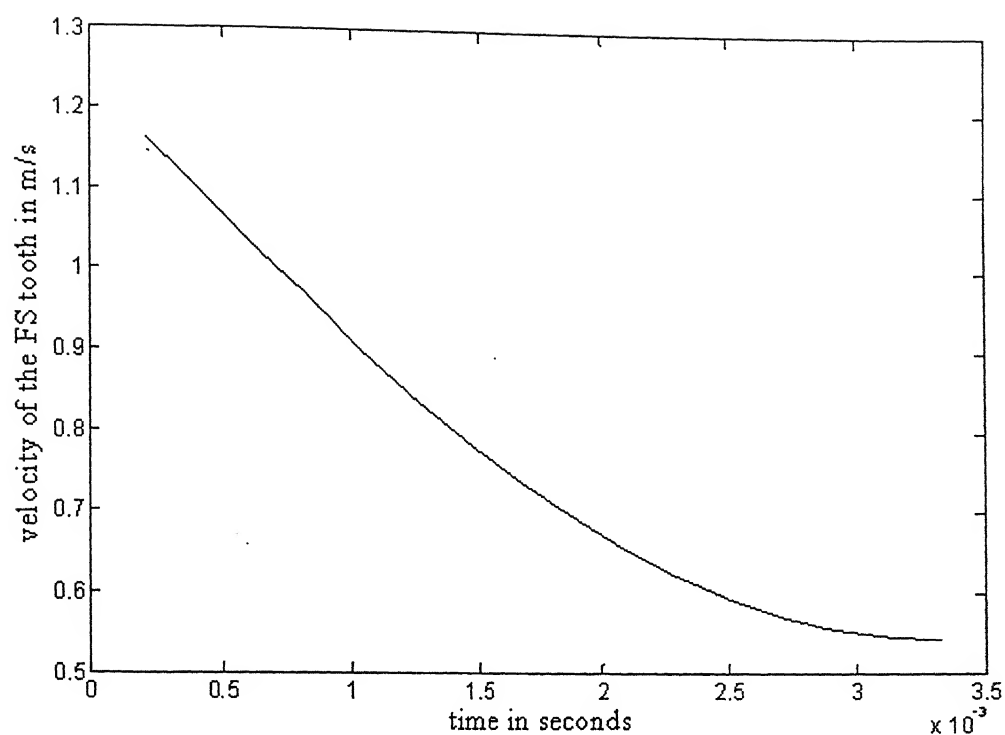


Fig. 24(b) Velocity of the FS tooth at the input speed 1500 rpm

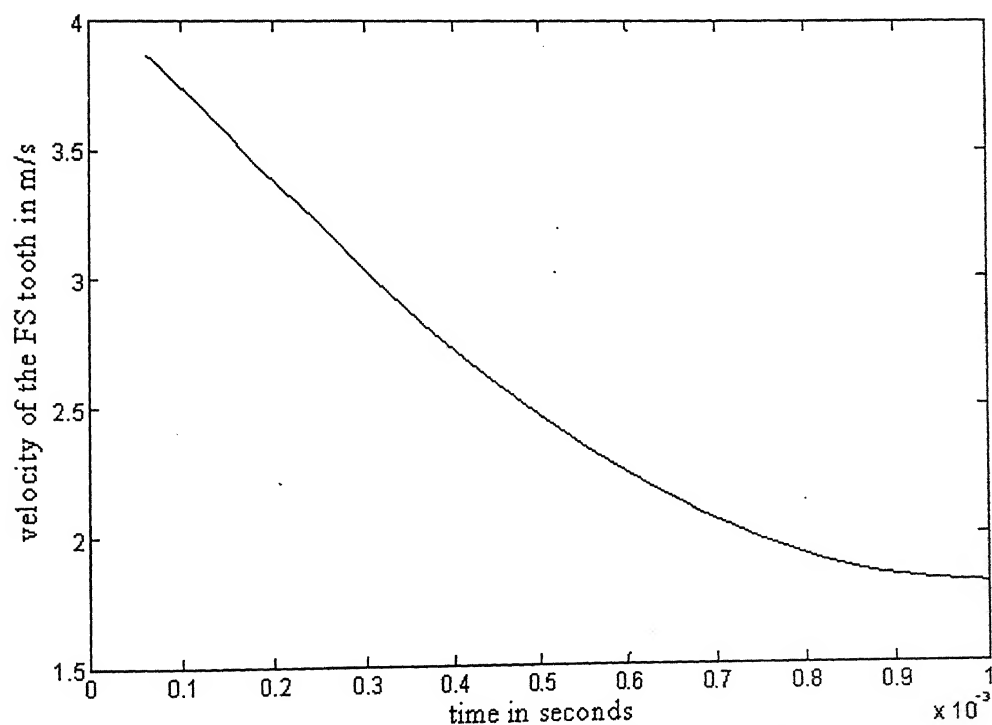


Fig. 24(c) Velocity of the FS tooth at the input speed 5000 rpm

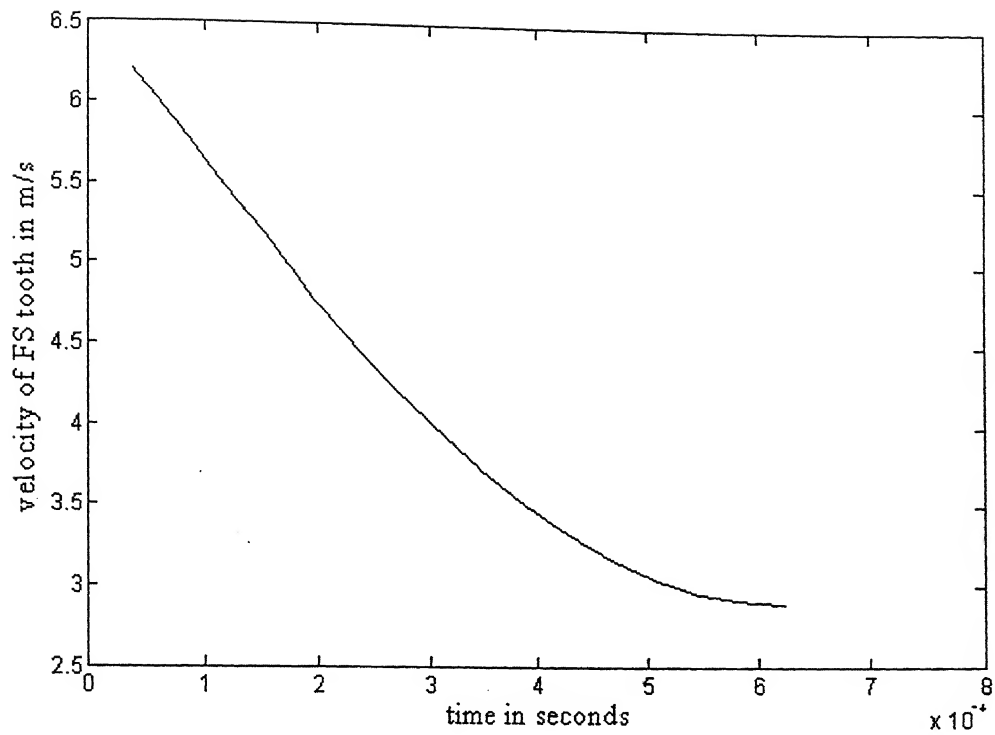


Fig. 24(d) Velocity of the FS tooth at the input speed 8000 rpm

Velocity profile in the case of involute profiles (gear ratio = 25)

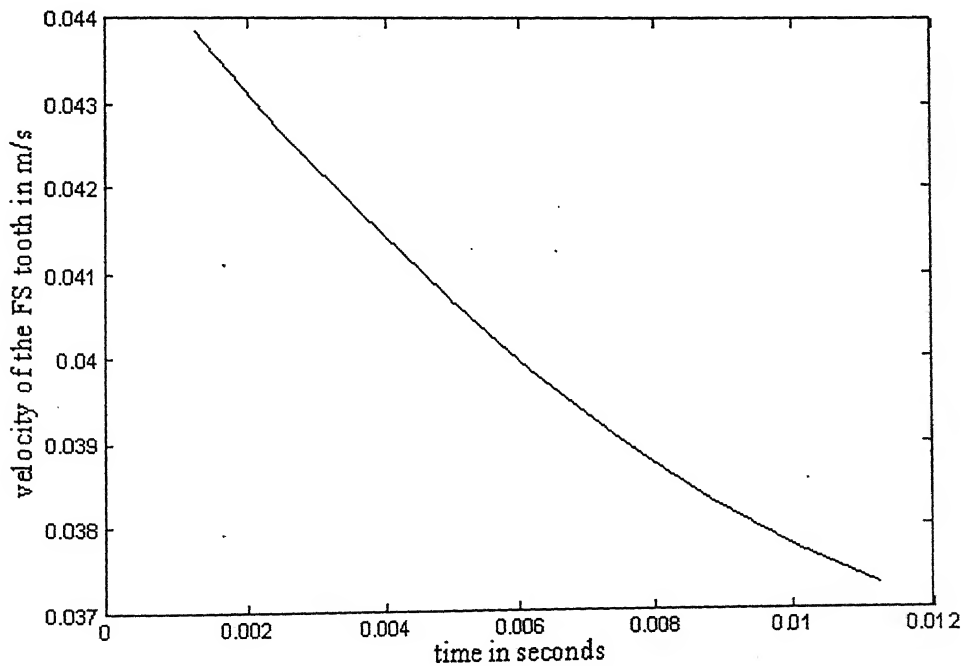


Fig. 25(a) Velocity of the FS tooth at the input speed 100 rpm

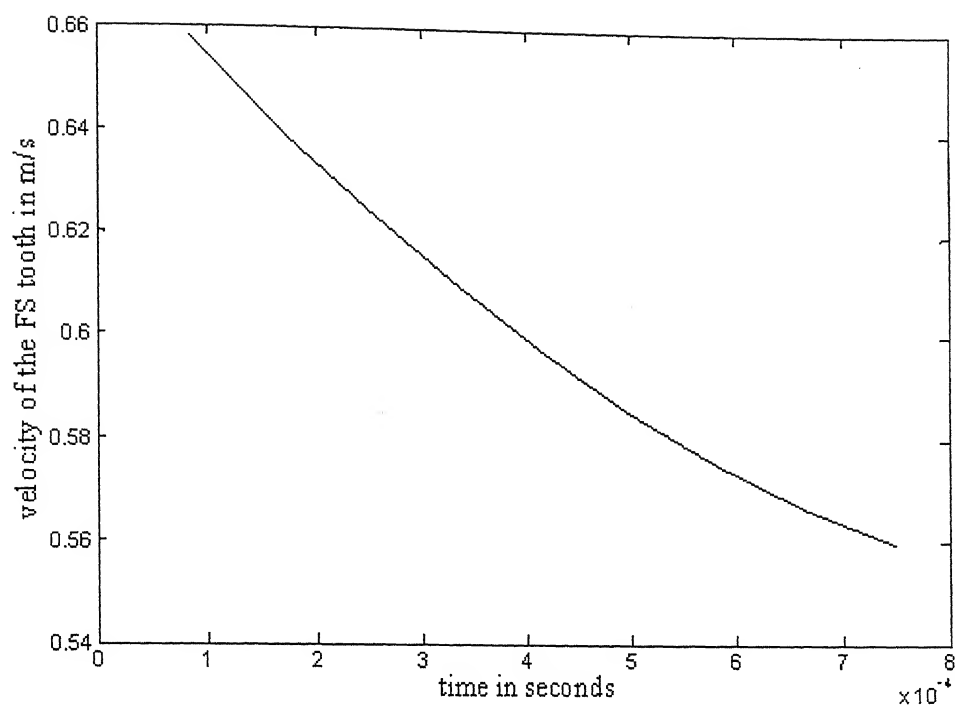


Fig. 25(b) Velocity of the FS tooth at the input speed 1500 rpm

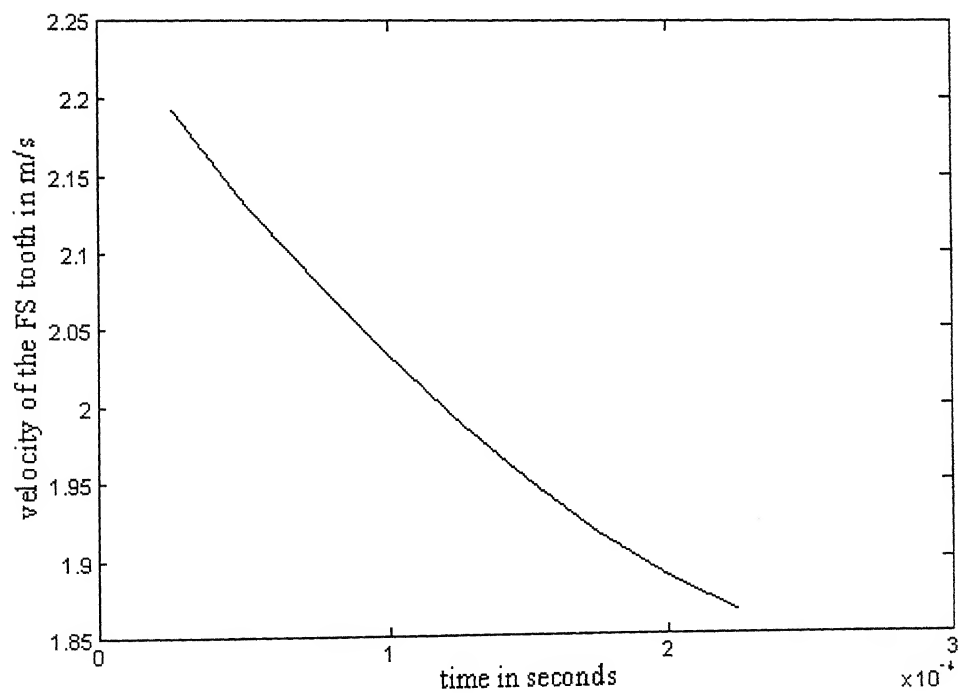


Fig. 25(c) Velocity of the FS tooth at the input speed 5000 rpm

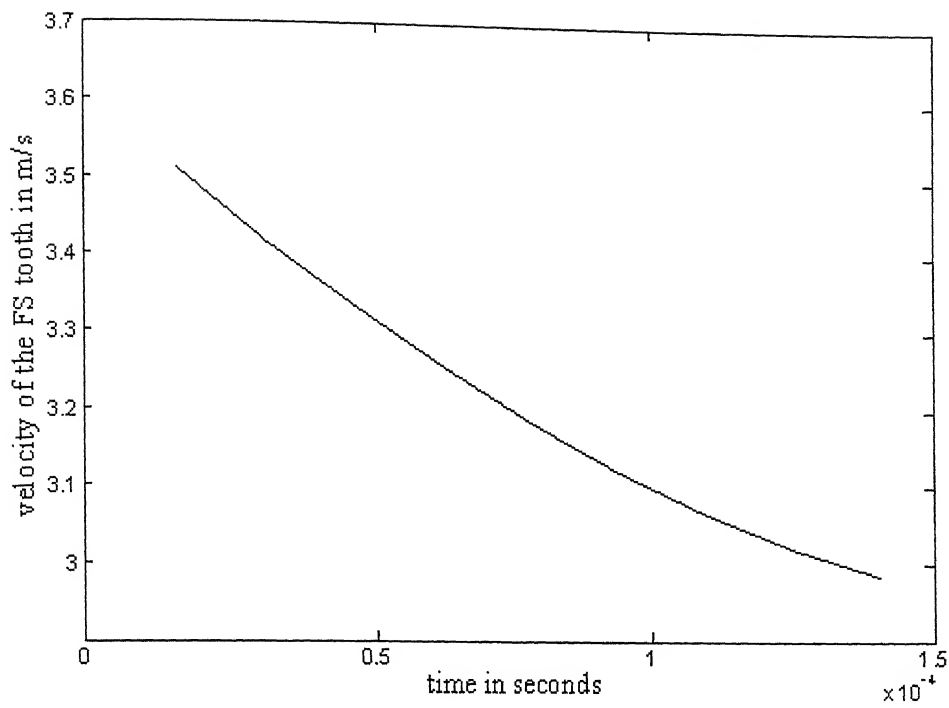


Fig. 25(d) Velocity of the FS tooth at the input speed 8000 rpm

#### Velocity profile in the case of involute profiles (gear ratio = 100)

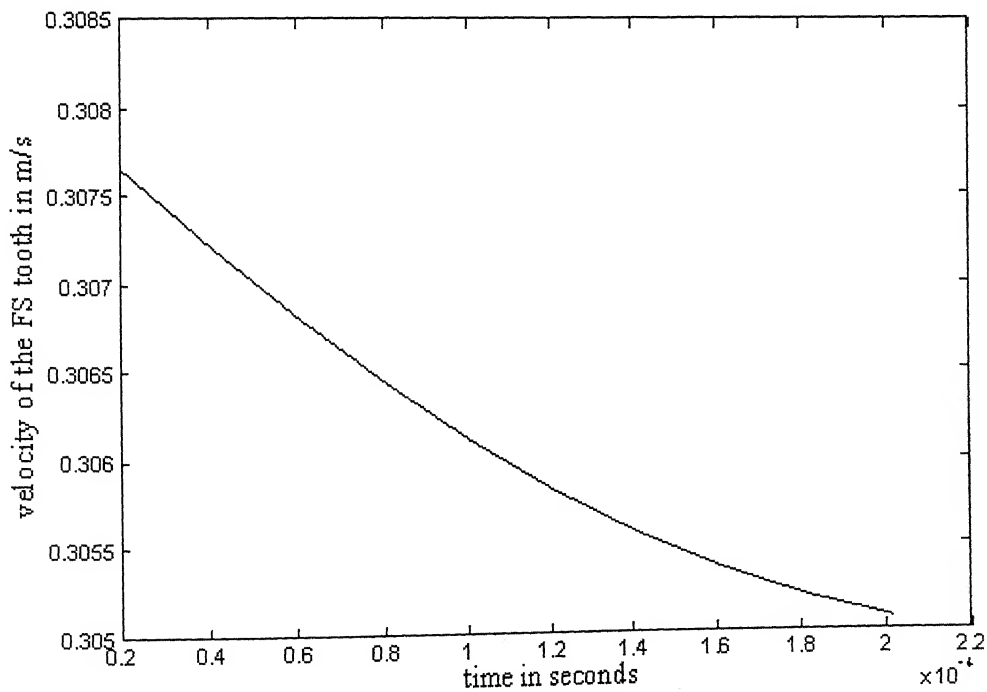


Fig. 26(a) Velocity of the FS tooth at the input speed 1500 rpm



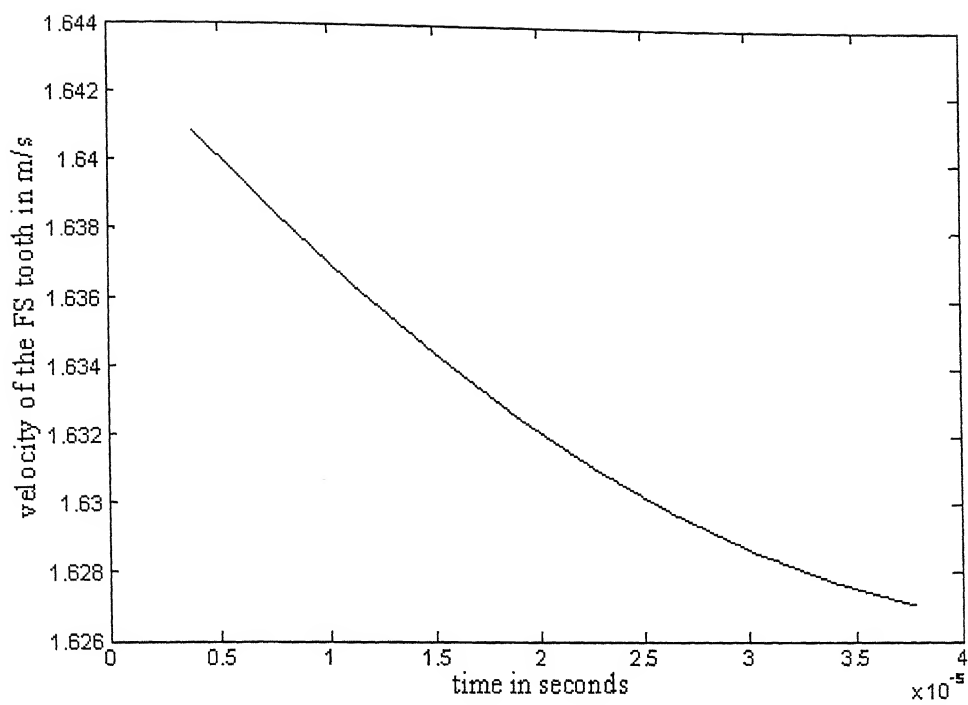


Fig. 26(b) Velocity of the FS tooth at the input speed 8000 rpm

# Chapter 4

## Contact Stresses

A finite element analysis has been carried out with ABAQUS for ascertaining the maximum stresses generating in the teeth during their contact. Hertz theory can be used to determine the stresses in the contact region. Hertz's theory yields stresses, deformations and the shape of the interface formed at two contacting bodies.

For very accurate results, it is necessary to find the stresses by dynamic analysis. Since the magnitudes of the velocities of the FS and the CS teeth are not very high, a static analysis can be performed by including the inertia forces acting on the teeth. But the mass of both the FS and the CS teeth is so less that the magnitude of the inertia forces (obtained by multiplying the mass with acceleration) can be negligible compared to the values of external loads that are acting at the interface of the teeth.

The normal load acting at the interface of the teeth and the kinetic frictional force are considered in this analysis. During the motion, the contact point on both the profiles and velocity of the FS tooth are changing. Since the frictional coefficient is taken as a function of sliding velocity, the kinetic frictional force acting at the interface is not constant.

The stresses are being ascertained by considering both the FS and the CS as elastic bodies. Even though both the FS and the CS are made of steel, the value modulus of elasticity is taken slightly less for the FS material by giving due consideration to its flexibility. The values of modulus of elasticity for the CS and the FS are  $2.3 \times 10^5$  MPa and  $1.95 \times 10^5$  MPa respectively. These stresses are found at the output torque of 70 N-m and at the input speed of 1200 rpm. The diameter of the CS is 200mm.

Han Su Jeon and Se Hoon Oh [12] studied the stress, the deformation and the related vibration characteristics using the finite element method on the FS as a part of speed reducer. They concluded that the stress in the circumference is five times greater than the radial stress. In their analysis Hertz stresses in the teeth are not reported.

The stresses are calculated for the synthesized teeth profiles and the involute teeth profiles. For the same resisting torque, the force acting on the teeth in the drives with synthesized profiles is less because of many number of teeth are in contact. In this analysis the magnitude of the force acting on the teeth is taken equal for both the synthesized and the involute teeth profiles.

4.1 Hertz Stress at the teeth contact of drives with the involute profiles

The stress results for the involute teeth profiles are shown at three positions, at the time of starting, at the mid point and at the end of the engagement. The legend shows the stress distribution.

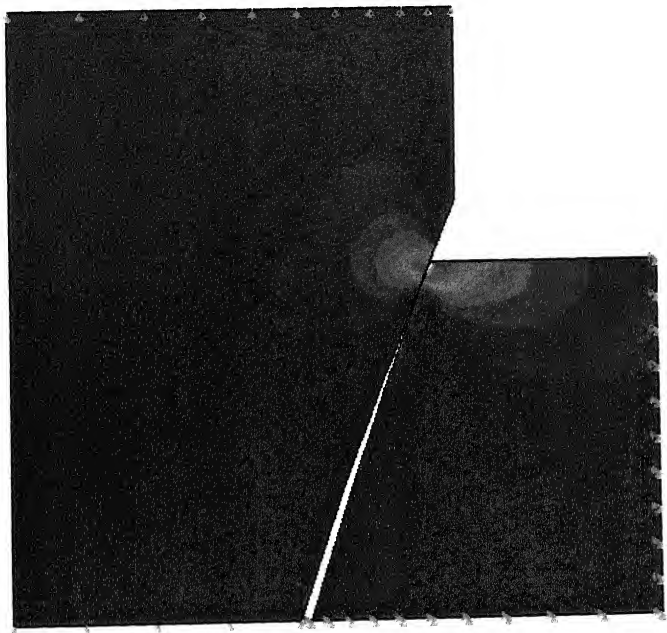


Fig. 27(a) The contact between the FS and the CS teeth at the start of engagement

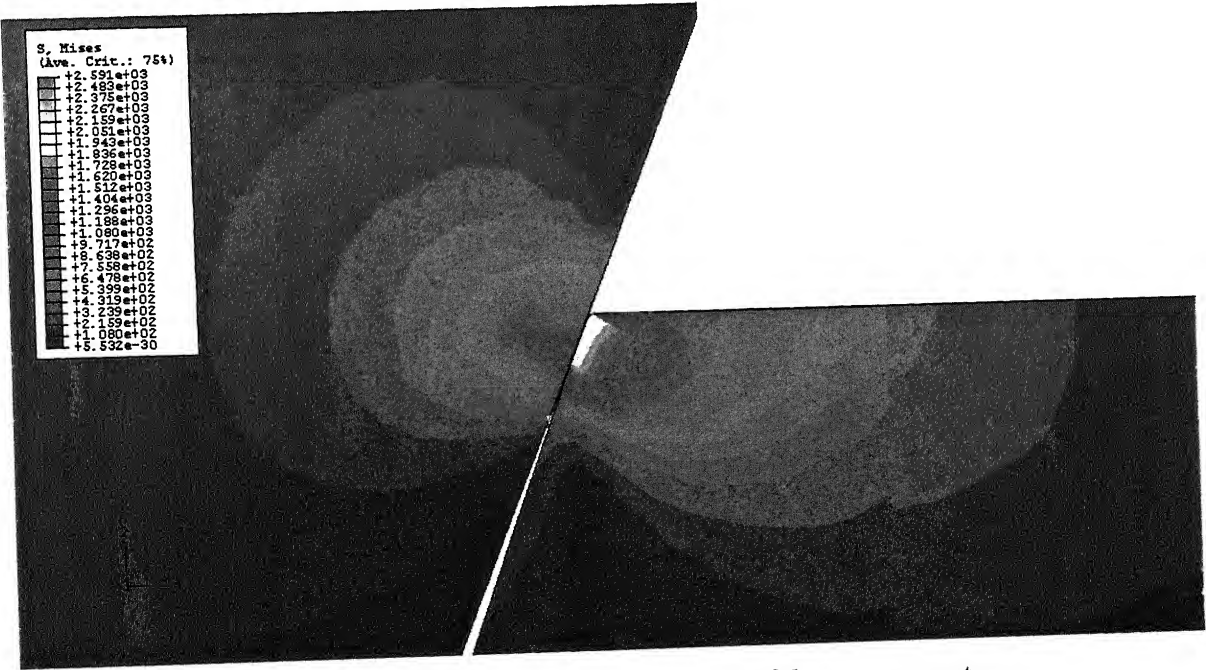


Fig. 27(b) Stress distribution at the start of the engagement

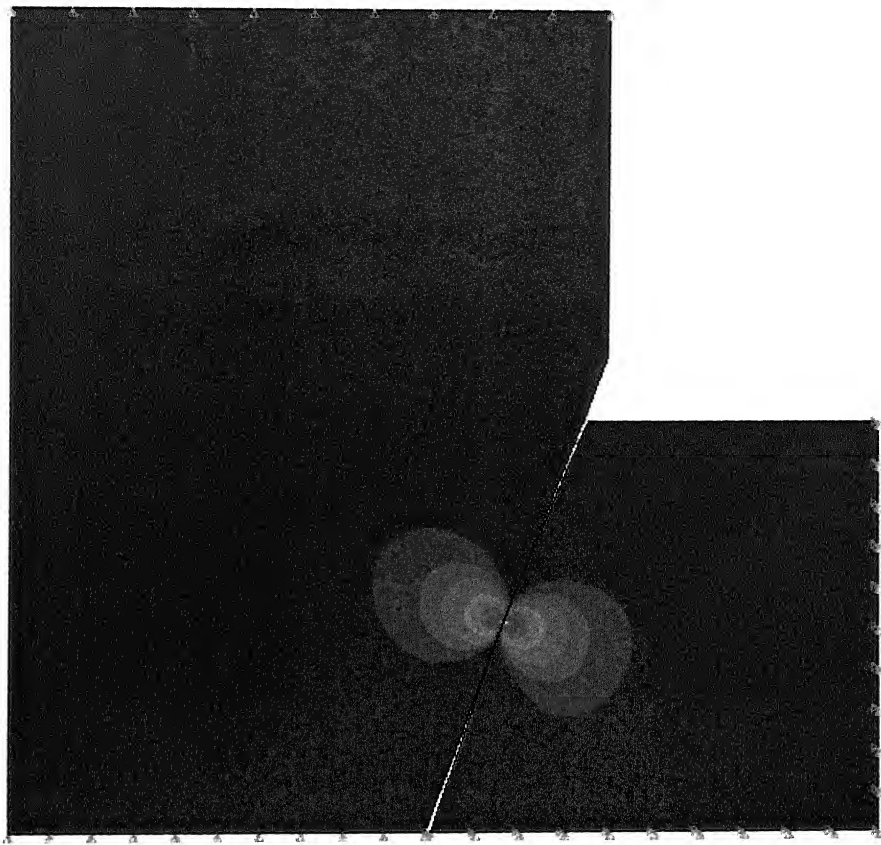


Fig 27(c) The contact between the FS and the CS teeth at the middle of the engagement

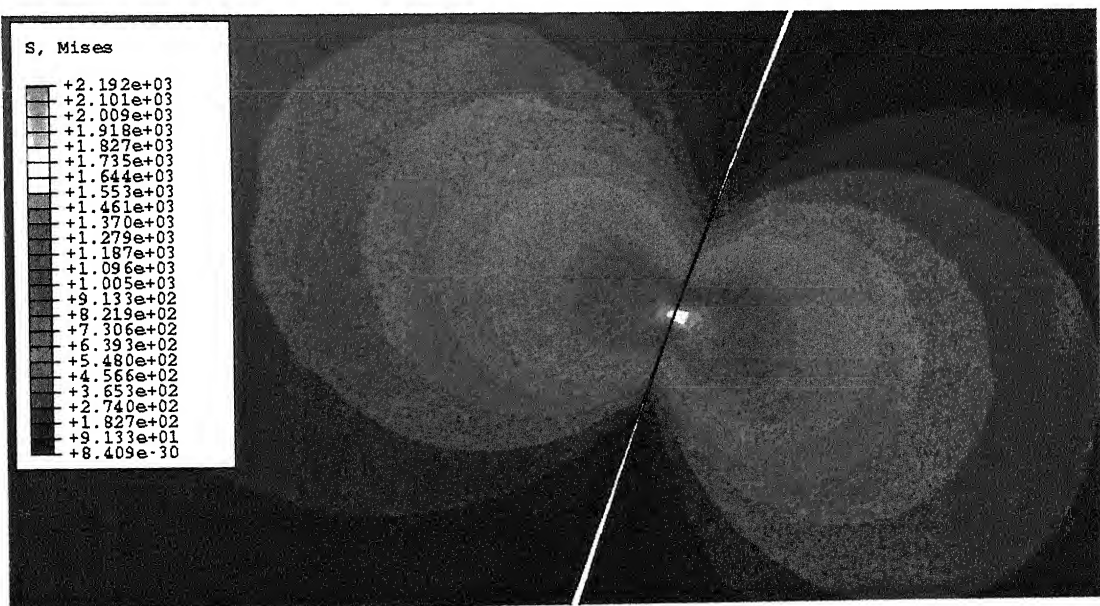


Fig. 27(d) Stress distribution at the middle of the engagement

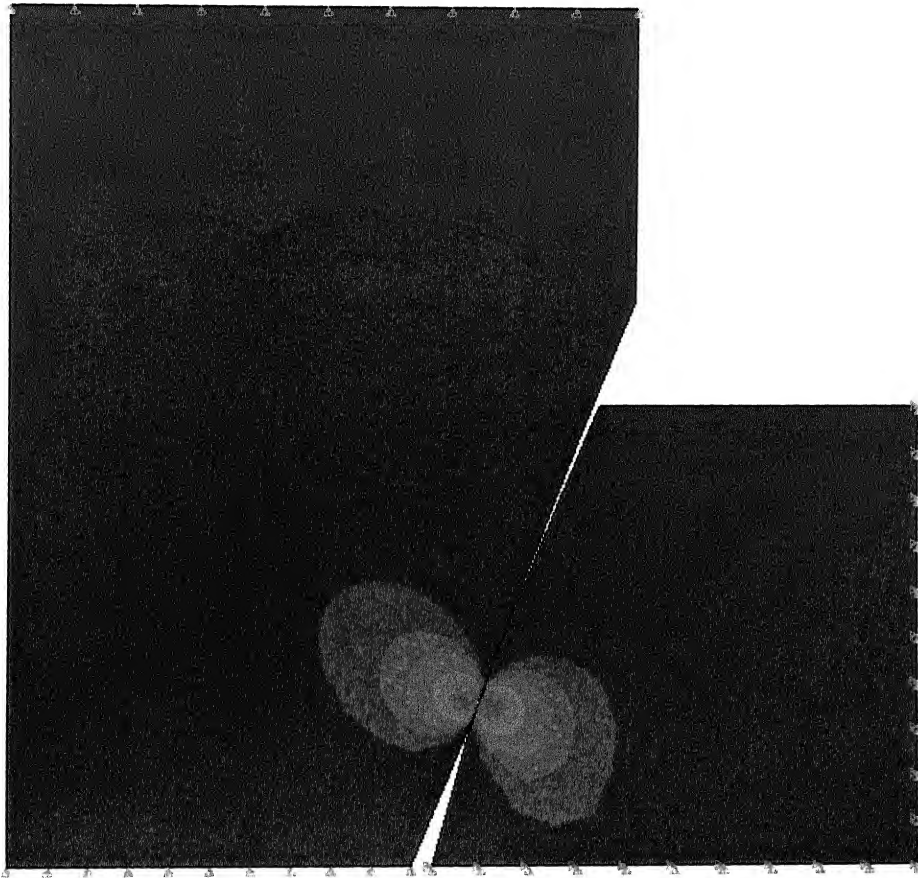


Fig. 27(e) The contact between the FS and the CS teeth at the end of the engagement

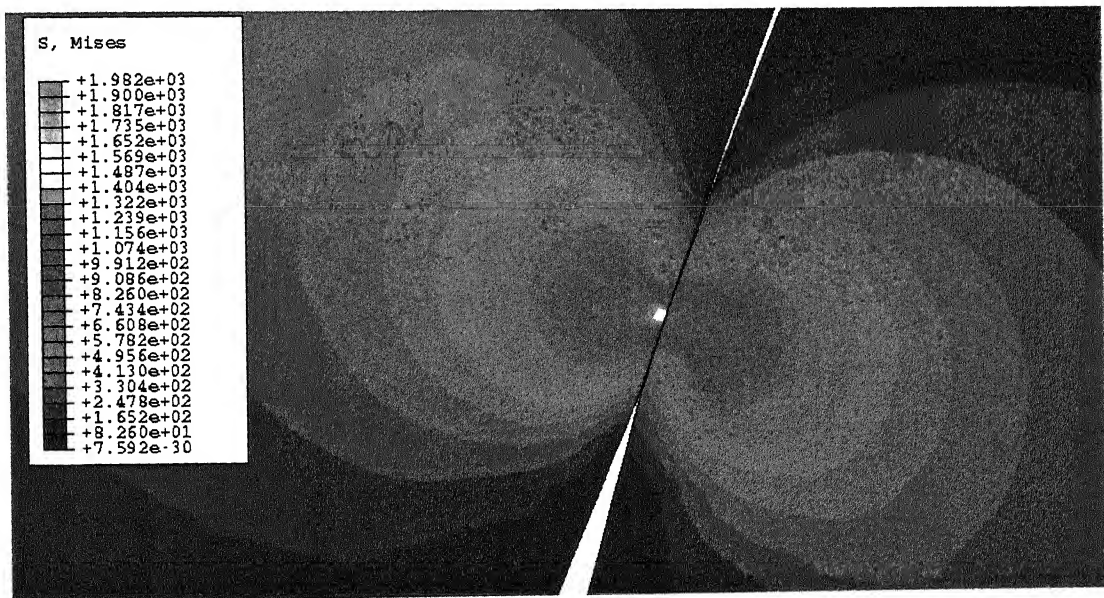
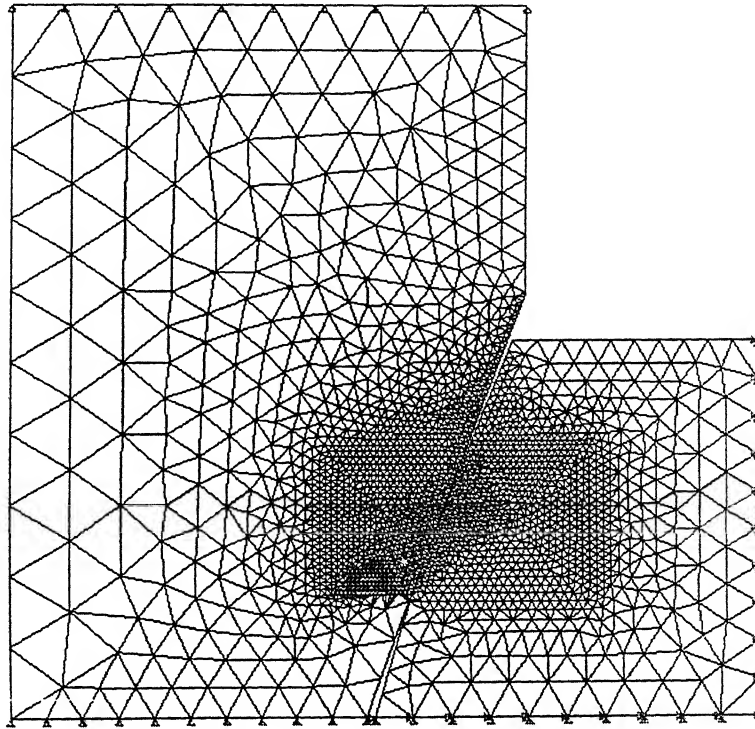


Fig. 27(f) Stresses distribution at the end of the engagement

Since the FS is assumed to have high torsional stiffness, its teeth are fixed and only the radial displacement of the CS is arrested. The load applied on the CS is calculated from the given torque.

Example of meshing pattern for the involute teeth





#### 4.2 Hertz stress at the teeth contact of drives with the synthesized profiles

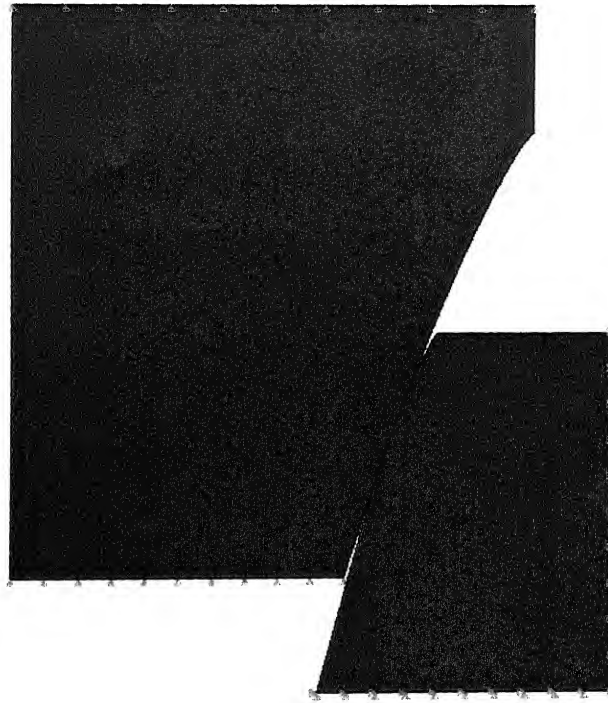


Fig 28(a) The contact between the FS and the CS teeth at the starting of the engagement

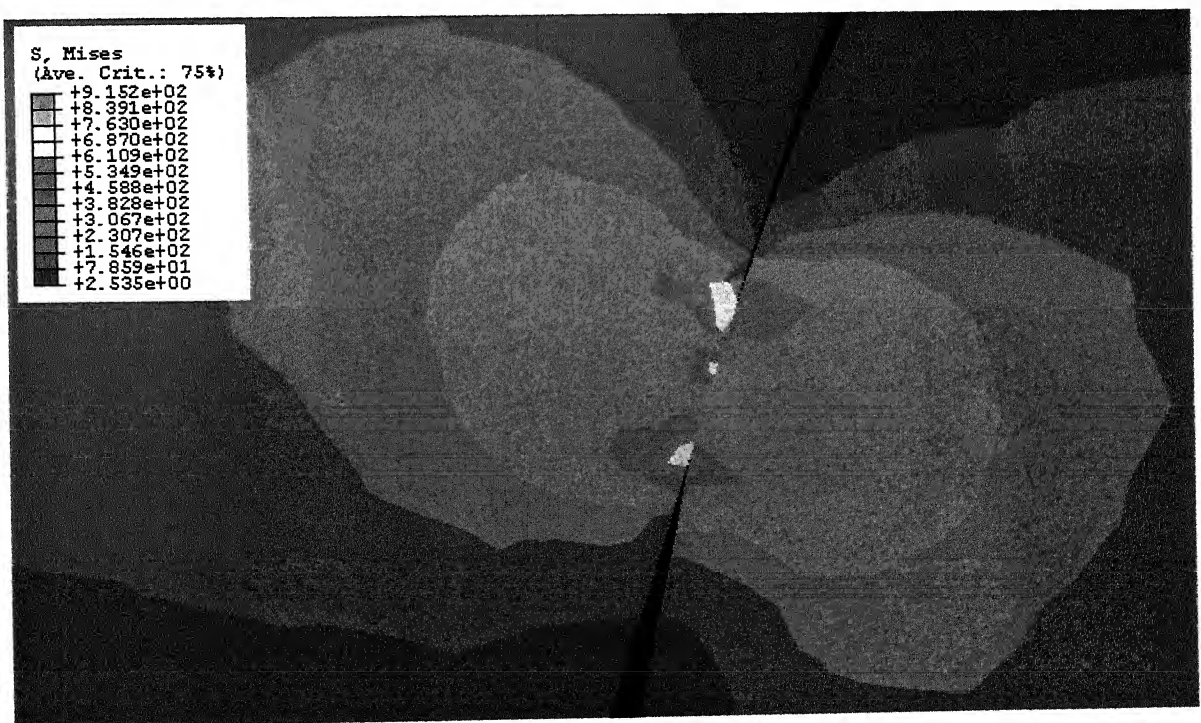


Fig 28(b) Stress distribution at the start of the engagement

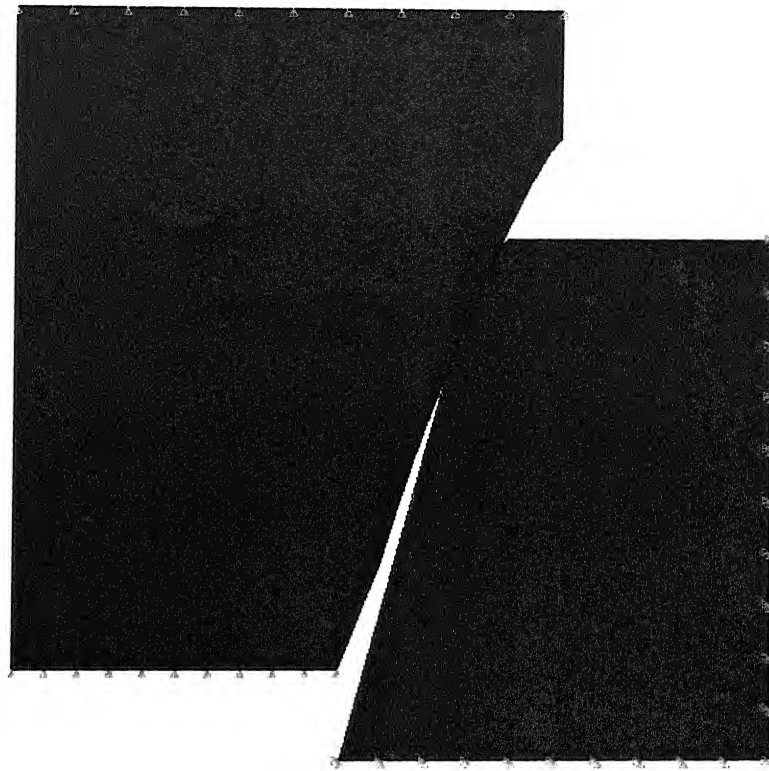


Fig. 28(c) The contact between the FS and the CS teeth at the middle of the engagement

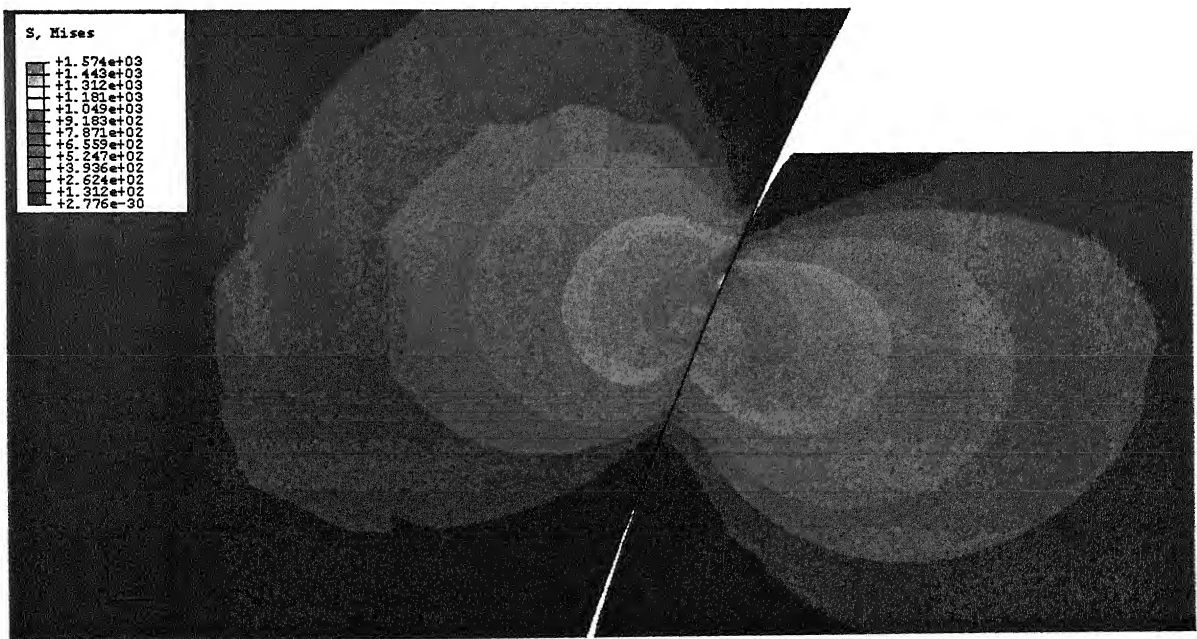


Fig. 28(d) Stress distribution at the middle of the engagement



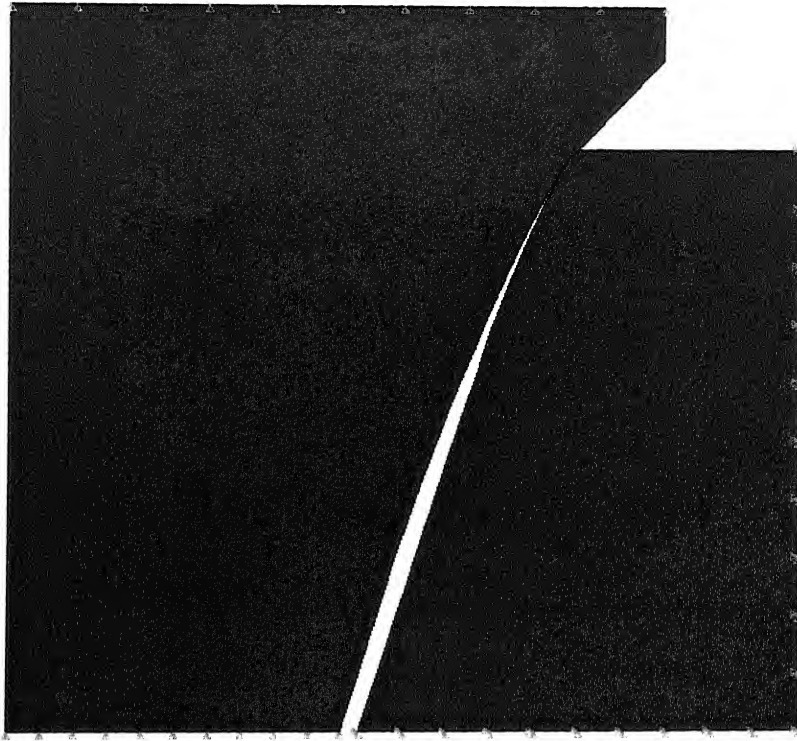


Fig. 28(e) The contact between the FS and the CS teeth at the end of the engagement

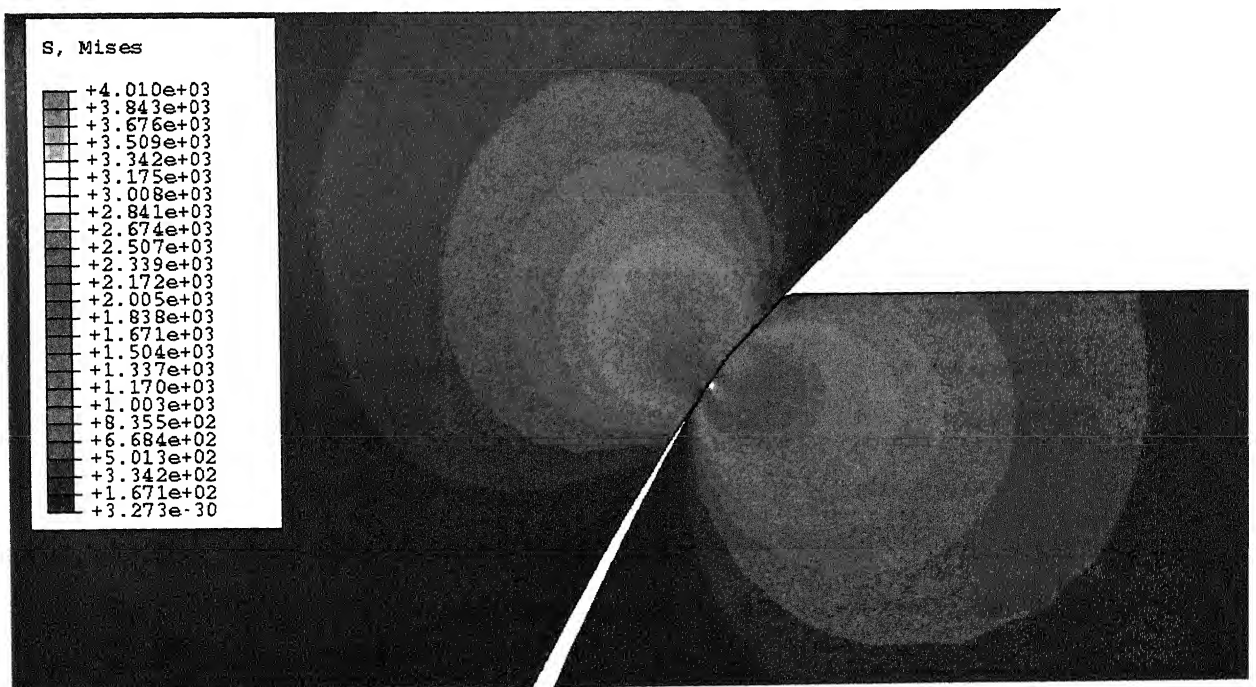
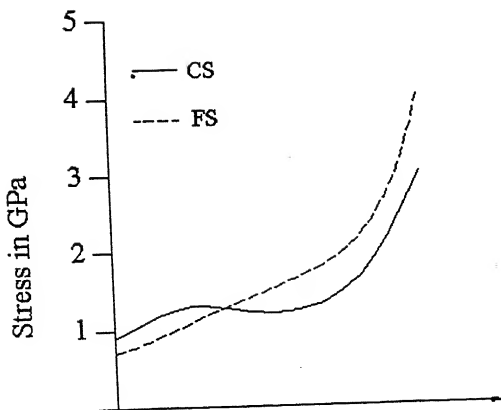
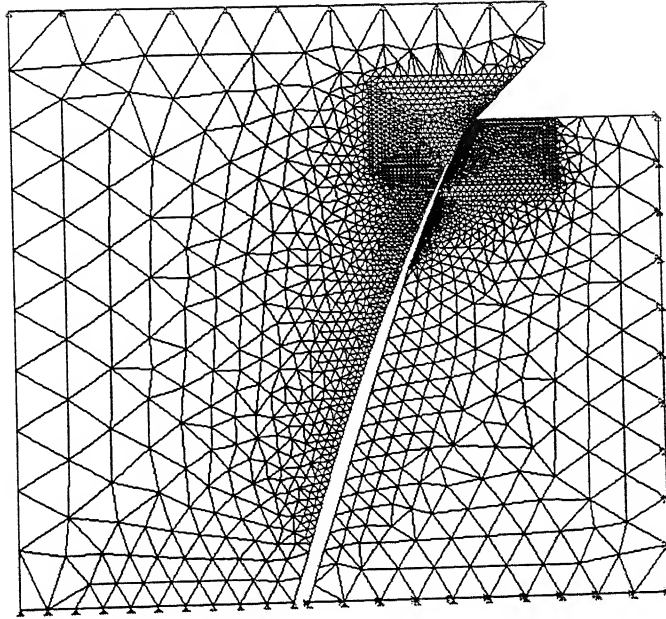


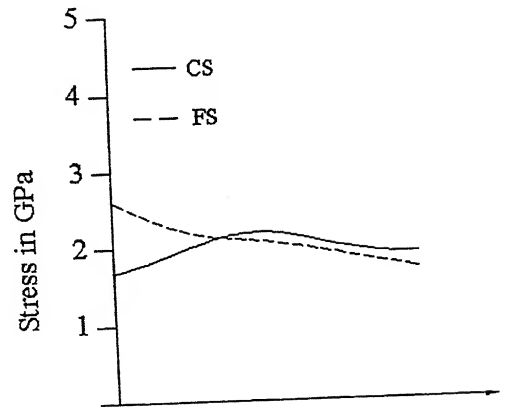
Fig. 28(f) Stress distribution at the end of the engagement

Example of meshing pattern for the synthesized teeth



From the start to the end  
of teeth engagement

(i) Synthesized profile



From the start to the end  
of teeth engagement

(ii) Involute profile

Fig. 29 Variation of contact stresses in the FS and CS

The stress distribution curves showing the stresses in the teeth of the FS and the CS for both the synthesized and the involute profiles are shown in Fig. 29.

# Chapter 5

## Concluding Remarks

### On the kinematic error

The kinematics of harmonic drives is analyzed. The theoretical kinematic error of the harmonic drive with involute tooth profiles on both the CS and the FS is studied. The drives with synthesized profile will have less kinematic error compared to drives with involute profile. The kinematic error is more pronounced for lower transmission ratios. Increasing the number of teeth and the difference in the number of teeth can reduce kinematic error. The given methodology is expected to decrease the dependency of the kinematic error on the number of teeth.

### On the life of the teeth profiles

In case of drives with involute profile, the contact lengths on the CS and the FS teeth are limited to low values. The contact ratio is also less. But with synthesized profiles, the lengths of the profiles subjected to teeth action are increased. The contact ratio is considerably higher. Thus the number of teeth that share the resistive torque is large. These two factors can increase the life of the drive.

### On the geometry of the teeth profiles

When the shape of the WG is not modified, the geometry of the teeth profiles obtained are shown in Fig. 17. Since the slope of these profiles is less i.e. the pressure angle is high, which will increase the magnitude of the radial component of the contact force. Since the Hertz stresses in both the FS and the CS teeth are directly related to the contact pressure, it is suggested that the slope of the profiles should be as high as possible.

### On the mechanical efficiency

In the normal operating speed range of the harmonic drive (500 – 1500 rpm) the rate of increase in mechanical efficiency decreases with speed. On the other hand, at very high speeds the mechanical efficiency starts decreasing. As the gear ratio increases, due to increase in teeth contact losses, the mechanical efficiency decreases.

### On the Hertz stresses

From the results obtained by the finite element analysis, it is concluded that the magnitude of the stress value is high at the end of the teeth compared to the base of the teeth. The increase in stresses in the synthesized profiles can be attributed not only to change in the radius of curvature

but also to increase in the effect of friction due to decrease in velocity. The effect of friction manifests in shifting of the maximum stress towards the surface which otherwise exists at certain depth below the surface.

## References

- [1] Istomin, S.N., and Borisov, S.G., 1983, "Calculation OF Kinematic Error of Harmonic Drives," Vestnik Mashinostroeniya, Vol. 63, Issue 2, pp.24-26
- [2] Emel'yanov, A.F., et al., 1983, "Calculation of The Kinematic Error of a Harmonic Drive Gear Transmission Taking into Account The Compliance of Elements," Vestnik Mashinostroeniya, Vol. 63, Issue 7, pp.9-12
- [3] Popov, P.K., et al., 1987, "Calculation of The Critical Speeds of a Drive with Harmonic Gear Transmission," Vestnik Mashinostroeniya, Vol. 67, Issue 3, pp.19-21
- [4] Ivashov, E.N., AND Nekrasov, M.I., 1984, "Calculation of The Wear of Harmonic Drives," Vestnik Mashinostroeniya, Vol. 64, Issue 1, pp.24-26
- [5] Rathindranath Maiti., 2004, "A Novel Harmonic Drive With Pure Involute Tooth Gear Pair," Transactions of the ASME, Vol. 126, pp. 178-182.
- [6] Hsia, L.M., 1988, "The Analysis and Design of Harmonic Drives," Proceedings of the 1988 IEEE International Conference on systems, man and cybernetics, pp. 616-619
- [7] Kiyosawa, Y., Ishikawa, S., and Sasahara, M., 1989, "Proceedings of The 1989 International Power Transmission and Gearing Conference".
- [8] Kondo, K., and Takada, J., 1987, "Study of Wave Gear Drives," JSME International Journal, Vol. 30, No. 263, pp. 854-860.
- [9] Ghorbel, F.H., Gandhi, P.S., and Alpeter, F., 2001, "On The Kinematic Error of Harmonic Drives," ASME Journal of mechanical design, Vol.123, March 2001, pp.90-97
- [10] Buckingham, E., 1963, "Analytical Mechanics of Gears," Dower publications, Inc., New York
- [11] Timothy D. Tuttle, 1992, "Understanding and Modeling the behavior of a Harmonic Drive Gear Transmission," AI-TR 1365, MIT Artificial Intelligence Laboratory.
- [12] Han Su Jeon and Se Hoon Oh, 2000, "A Study on Stress and Vibration Analysis of a Steel and Hybrid Flexspline for Harmonic Drive," Composite Structures, Elsevier Science Limited, Vol. 47, pp. 827-833
- [13] Merritt, H.E., 1962, "Gears," Sir Isaac Pitman & Sons Ltd, London.

## Appendix I

Program for calculating efficiency written in MATLAB 7.01

Values of  $r$

```
R=[101
    101.350594
    101.669419
    101.977049
    102.259885
    102.519913
    102.755423
    102.972056
    103.170468
    103.349553
    103.510611
    103.652957
    103.775937
    103.880685
    103.96622
    104.030355];
```

Values of  $d$

```
D=[0.242029
    0.228512
    0.214055
    0.201217
    0.186969
    0.174804
    0.163855
    0.153845
    0.144859
    0.136836
    0.129785
    0.123779
    0.118956
    0.11552
    0.113683
    0.112864];
```

Values of  $\phi$

```
PHI=[103.20179
    106.01252
    105.79144
    107.38581
    110.32724
    293.17688
    116.25645
    299.74341
    123.56178
    127.80114
    132.5284
    137.83801
    143.76707
    150.37406
    337.57464
    165.33095];
```

```
shi=1.875*pi/180;
```

```

values of  $\theta$ 
th=[71.9532
    71.58
    70.1085
    69.171
    68.6136
    67.915
    67.1782
    66.422
    65.577
    64.63
    63.5277
    62.203
    60.515
    58.1883
    54.557
    46.8] ;
L=0;
rho=25;
E=[];
NN=[];
n1=0;
for y=1:1:150
n1=n1+10;
t=(shi*180/pi)/(n1*6);
    tout=400;
        for i=1:1:16
            r=R(i)/1000;
            x=r*shi/rho;
f0=tout/r;
d=D(i)/1000;
vf=d/t; velocity of the flexspline tooth
vc=x/t; velocity of the CS
phi=PHI(i);
vs=sqrt(vc^2+vf^2-2*vf*vc*cos(phi*pi/180)); sliding velocity
vs1=vs*196.848;
mu=0.2/(exp(0.17*sqrt(vs1)))+0.0013*sqrt(vs1)+0.02;
p=f0/(sin(th(i)*pi/180)-mu*cos(th(i)*pi/180));
l=mu*p/4*vs*t;
L=L+l; enegy loss
end
n2=n1/rho;
ef=(tout*n2*t^4)/(tout*n2*t^4+2*L);
E=[E;ef];
NN=[NN;n1];
L=0;
end
plot(NN,E,'color','r')
hold on

```